BNL--51864

DE85 010698

HEAT/MASS FLOW ENHANCEMENT DESIGN FOR A METAL HYDRIDE ASSEMBLY

FINAL REPORT

Prepared by

Southern California Gas Company
810 South Flower Street
Los Angeles, California 90017

Solar Turbines, Inc.
P.O. Box 809666
San Diego, California 92138

T.A. Argabright

February 1985

Prepared for the
ENERGY APPLICATIONS AND ANALYSIS DIVISION
DEPARTMENT OF APPLIED SCIENCE
UNDER SUBCONTRACT NO. 534098-S

BROOKHAVEN NATIONAL LABORATORY
ASSOCIATED UNIVERSITIES, INC.
UPTON, LONG ISLAND, NEW YORK 11973

UNDER CONTRACT NO. DE-AC02-76CH00016 WITH THE
UNITED STATES DEPARTMENT OF ENERGY

TABLE OF CONTENTS

TABLE OF CONTENTS (Continued)

LIST OF FIGURES

LIST OF FIGURES (Continued)

LIST OF TABLES

ABSTRACT

Southern California Gas Company and Solar Turbines Incorporated are cooperating in the development and demonstration of a metal hydride/chemical heat pump (MHHP). In the design of the MHHP, heat transfer was considered to be the key technical study area. The goal of this effort is improved heat transfer and reduced thermal mass in a hydride heat exchanger/containment assembly.

Phase I of the three phase development program resulted in the detailed design of an advanced hydride heat exchanger. Phase II consisted of the experimental verification of the hydride alloy design data, fabrication of the hydride heat exchanger module components, heat transfer testing of a single heat exchanger element and preliminary performance testing of the entire module. Phase III was devoted to the complete characterization of the hydride heat exchanger modules through further operation and testing. A review of other possible hydride heat transfer concepts was also conducted in Phase III. The work described in this report was accomplished in Phase III.

GLOSSARY OF TERMS

BNL	Brookhaven National Laboratory
SoCal	Southern California Gas Company
Solar	Solar Turbines Incorporated
Mm	Mischmetal
WSA	Warm Side Alloy
CSA	Cold Side Alloy
MHHP	Metal Hydride Heat Pump
WSV	Warm Side Vessel
CSV	Cold Side Vessel
COP	Coefficient of Performance
TMR	Thermal Mass Ratio

NOMENCLATURE

Symbol	Description
T_H	high temperature, °F (firing)
T_M	medium temperature, °F (sink)
T_L	low temperature, °F (refrigeration effect)
COP	Coefficient of Performance
Q	quantity of heat, Btu/hr
TMR	thermal mass ratio
t	time, minutes
SH	sensible heat, Btu/°F
ΔP	pressure drop, psi
C_p	specific heat, Btu/lb°F
ΔT	temperature change, °F
V	volume, cubic inches
m	mass flow rate, gpm
q	heat, Btu
ΔH_f	heat of formation, Btu/lb
ϱ	density, lb/in^3

BNL PERSPECTIVE

The work reported here concludes the three-phase effort on developing an improved metal-hydride chemical heat pump. In Phase I, the effort included development of the conceptual design and transient-heat-transfer models, laboratory verification of design and material performances, as well as a study of the potential applications and market sectors. The key accomplishment was design of an efficient finned-tube heat exchanger for enhancing heat/mass transfer in a hydride bed. This work is documented in BNL 51539, February 1982.

Logically, the work done in Phase II (BNL 51727, September 1983) consisted of experimental verification of the hydride-alloy design data, fabrication of the heat-exchanger-module components, testing of a single heat exchanger tube, and preliminary performance testing of the entire module. When testing showed that the performance was sub-normal, the fault was traced to the cold-side alloy which did not have the specified composition. This unexpected event led to extending the work to Phase III.

Because of a redirection of DOE's goal, with the change in federal administration policies toward more long-term research, it was anticipated that further development of the metal-hydride heat pump concept would be left to the private sector at the end of Phase II. However, it was decided to pursue a Phase III first so that the inferior alloy could be replaced and the system performance fairly characterized.

Replacement of the cold-side hydride alloy permitted much improved heat pump performance. By minimizing thermal losses to vessel components surrounding the hydride, performance can be further improved. Before such design revisions are made, however, the modules should be dismantled and inspected for any damage which could have been caused by hydride expansion, and to determine the extent of fin area not still immersed in hydride (due to bed settling). These tasks were not included in the contract work.

In discussing the configuration of a large heat pump, the contractor has wisely stated that modular construction would be used so that any module which becomes inoperable could be isolated and replaced without shutting down the entire system. Presumbably, scale-up would consist of increasing the module length and number of modules.

A complementary effort, and one which led to selection of the present design, was a qualitative evaluation, and some discussion, of various heat transfer concepts for seven practical characteristics. This tabulation of hydride/water/filter geometries and their interpretation of the characteristics serves as a guide to designers of heat exchangers for metal-hydride service. A configuration not included is finned-tube assemblies, such as used in automobile radiators, with the hydride contained in shallow plastic trays. A more detailed consideration of the various configurations should be made before selecting one for a particular application.

The effort expended in these three development phases has furthered hydrogen-hydride technology by providing a method for accurately predicting heat pump performance and by providing a workable hardware design which can be further optimized.

The information and experience derived from the development of a high-flux, low-mass tube for hydride heat exchangers represent a significant advancement pertinent to other rapid-cycling applications such as thermally-driven hydrogen compressors and hydrogen separation/recovery systems. Further pursuits will rely on private sector evaluation of commercialization prospects in light of current federal policy and budgetary guidelines which preclude DOE/BNL involvement.

1

EXECUTIVE SUMMARY

A metal hydride heat pump (MHHP) is an innovative chemical heat pump that utilizes the heat of reaction of hydrogen with selected metal alloys called hydrides. The alternating absorption and desorption of hydrogen into two different hydrides can be used to provide refrigeration, heat amplification or temperature upgrading without consumption of metal or hydrogen gas. This can occur because metal hydrides have the ability to undergo a reversible thermal decomposition which is exothermic when the hydride is absorbing hydrogen and endothermic when desorbing. The MHHP can be tailored to operate over a wide range of input and ambient temperatures and can thus be used with a variety of heat sources including waste heat, solar energy or a fossil fuel.

In 1980, Brookhaven National Laboratory (BNL) requested proposals to advance the heat transfer technology within the metal hydride heat pump. This was to be accomplished by the development of a high heat transfer, low thermal mass hydride containment device. Southern California Gas Company (SoCal) and Solar Turbines Incorporated (Solar) prepared the winning proposal for this current effort based on their extensive development experience with metal hydrides and heat exchanger technology gained in earlier and on-going private efforts. SoCal has entered into this effort because of its strong interest in bringing new energy conserving products to the marketplace. Solar can envision the MHHP as a potential energy recovery device for its line of gas turbine engines. With this effort, the state-of-the-art of the MHHP is being further advanced for the benefit of the nation as well.

This current development effort has progressed through three phases. The work described in this report was accomplished in Phase III. The scope of Phase I included the development of the conceptual design for the metal hydride heat pump, a study of the potential applications and market sectors, laboratory verification of design and material performance and development of transient heat transfer models. Phase I resulted in the detailed design of an advanced hydride heat exchanger. Phase II consisted of the experimental verification of the hydride alloy design data, fabrication of the hydride heat exchanger module components, heat transfer testing of a single heat exchanger element and preliminary performance testing of the entire module. Phase III was devoted to the operation and testing of this device and a review of other hydride heat exchanger designs.

In the design of the MHHP, heat transfer is considered to be the key technical study area. The MHHP is a cyclical device, therefore, rapid heat transfer allows more cycles per hours and a greater productive thermal capacity per pound of hydride powder. This is a critical parameter as the cost of the hydride powder is the primary expense in the heat pump. It is imperative to

minimize the quantity of hydride per useful output. High heat transfer leads to rapid cycling, high capacity and, consequently, low hydride inventory per useful output and lower system costs.

High heat transfer can be easily accomplished with massive, large surface area heat exchangers, however, since the heat exchanger must follow the cyclic temperatures of the MHHP, its mass is parasitic. These self-heating and cooling thermal losses to the heat exchange structure must be minimized; therefore, the goal was to provide the high heat transfer with a low mass unit.

The final hydride heat exchanger design embodies the best features of extensive computer modeling and experimental verifications. SoCal and Solar have produced a state-of-the-art hydride heat exchanger design which:

- increases heat transfer
- lowers the cycle time
- improves thermal capacity
- reduces sensible heat losses and water inventory
- reduces the amount of hydride powder necessary per useful output
- optimizes particle containment and minimizes the required surface area of the (expensive) filter material
- minimizes the seal areas
- lowers the total cost per useful output.

The hydride heat exchangers were constructed in Solar's Research Laboratories. The modules consist of two cylindrical pressure vessels connected as a pair. One vessel contains hydride $LaNi_5$ packed around 14 finned copper tubes, while the second vessel contains hydride $MmNi_{4.15}Fe_{0.85}$ in a similar configuration. Insulation thermally isolates the tubes and hydride materials from the high mass pressure vessel. A single metallic filter in each vessel prevents hydride migration from one vessel to another. The vessels are connected together with a hydrogen flow path. The heat transfer media, water, flows through the finned tubes.

Preliminary test results in Phase II indicated that the hydride heat exchangers functioned as predicted fulfilling development goals of increased heat transfer and lowered cycle time. It was also determined that the heat pump effectiveness was highly dependent upon the hydride utilization factors of the selected hydride alloys - $LaNi_5$ and $MmNi_{4.15}Fe_{0.85}$. Based on previous development work with hydride alloys, the assumed hydride utilization factor was 75 percent. This means that 25 percent of each metal hydride remains inactive (not absorbing hydrogen) due to contamination or incomplete activation. As a result of testing the hydride heat exchangers in the heat pump mode in Phase II, it was discovered that, although the $LaNi_5$ utilization

factor was 72 percent, the factor for the $MmNi_{4.15}Fe_{0.85}$ side was just 19 percent. The outcome of these circumstances was a lower output capacity in terms of refrigeration.

In Phase III, a new batch of $MmNi_{4.15}Fe_{0.85}$ hydride was loaded into the cold side hydride heat exchanger vessel and testing was continued. The resulting hydride utilization factors were 76.4% for the $LaNi_5$ side and 63.7% for the $MmNi_{4.15}Fe_{0.85}$. This development allowed for improved refrigeration performance and overall Coefficient of Performance (COP).

2

INTRODUCTION

2.1 PROGRAM BACKGROUND

The metal hydride heat pump (MHHP) is a concept that could result in an energy efficient technology driven by oil, natural gas, waste heat or solar energy. The MHHP could be part of a cogeneration system. In such a system, it would recover and utilize low grade waste heat. Some of the competitive advantages of the metal hydride heat pump include:

- operation on low grade heat
- gas or liquid heat exchange
- use of multiple energy sources in one unit
- environmentally acceptable
- compact
- variable shape and size according to application
- quiet operation
- simplicity - no moving parts
- potential for long life operation
- ability to tailor operation to available temperature source.

In the early 1970's Solar Turbines Incorporated (Solar) performed internal research to investigate potential heat utilization technologies. Metal hydrides were identified as a potential foundation for a thermally driven heat pump. The concept was verified by experimental work and proved to be very promising. In 1978, Southern California Gas Company (SoCal) entered into an agreement with Solar to accelerate the development of this new technology. SoCal entered into this agreement because of the large potential energy savings in their service area and because of SoCal's strong interest in investigating new energy conserving products. In 1980, Brookhaven National Laboratory (BNL) requested proposals for the development of a technology applicable to the MHHP for the benefit of the nation. This technology encompasses the design and development of a high heat transfer, low thermal mass hydride containment device. SoCal, with Solar as a subcontractor, submitted the winning proposal and embarked on this current effort. Figure 1 illustrates the project organization.

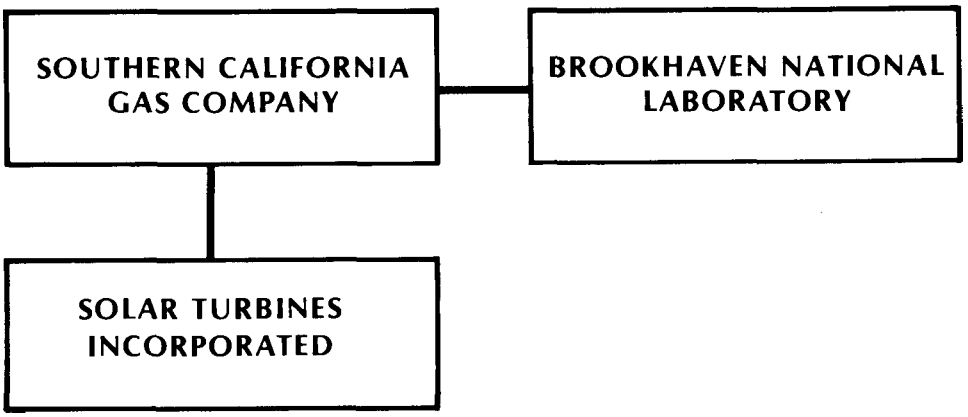

Figure 1. Project Organization

SoCal and Solar are cooperating in the development and demonstration of the MHHP. The MHHP is considered to have great potential as an energy conserving technology. Basically, the MHHP is a chemical heat pump containing two different metal hydrides. The concept utilizes the ability of selected metals to absorb and desorb hydrogen without the consumption of metal or hydrogen. The MHHP can be tailored to provide heating and/or cooling, or temperature upgrading over a wide range of temperatures and, thus, can be used with a variety of heat sources.

2.2 PROGRAM GOAL

The goal of this effort is the research, development and testing of a heat exchanger device for a metal hydride assembly. (The project scope did not include the optimization of the insulation, the pressure vessel body and the flange head.) The specific technical issues where development was required and emphasized to provide a technically sound design are outlined below:

Heat Transfer

The primary cost item in the heat pump is the metal hydride powder. AB_5 hydride alloys ($LaNi_5$ is a good example of an AB_5 alloy), the materials selected, cost $25/lb (1984$). Thus, it is imperative to minimize the quantity of metal hydride powder per useful output. This is accomplished by reducing the cycle time and minimizing the parasitic thermal losses to the structure of the heat pump. The cycle time is controlled by the heat transfer characteristics of the hydride heat exchanger. Since particle-to-particle heat transfer within the powdered metal hydride is extremely slow, it is necessary to enhance the transfer with a low mass, extended surface, heat transfer device imbedded in the powder. It is also important to minimize the mass of the structure to reduce the parasitic self-heating and cooling losses. Therefore, the goal was to provide high heat transfer with a low thermal mass heat exchanger.

- Performance

The performance of a hydride heat pump is expressed in terms of the Coefficient of Performance (COP) and the output capacity. The COP is a ratio of the net useful output energy to the required driving energy. COP values for the MHHP are maximized by minimizing parasitic losses -- the less energy required to heat and cool the heat exchanger structure, the more net useful output energy.

Similarly, the capacity of an MHHP is expressed in terms of the rate at which useful output energy is exchanged. It is calculated by dividing the energy output by the cycle time. Thus, cycle time is inversely proportional to capacity. A reduction in cycle time increases the capacity.

- Particle Containment

A filter is used to contain the metal hydride within each module and a large hydrogen pressure drop could occur unless the filter is properly designed and installed. A high pressure drop would slow the flow of hydrogen and increase the cycle time, thus increasing the amount of hydride material needed per useful output.

- Particle Expansion

The process of hydrogen absorption and desorption causes the metal crystal lattice to expand and contract leading to the comminution of the original hydride alloy particles. After many such cycles, the process of comminution produces a progressively greater proportion of fine particles. The MHHP must be designed with the ability to absorb this hydride powder expansion.

These issues were addressed via a three-phase approach (Fig. 2):

Phase I - Concept Definition

Phase II - Proof of Concept

Phase III - Heat Transfer Optimization

Phase I of this project was initiated in February 1981 and was completed in January 1982. The tasks of Phase I included the development of the conceptual design for the metal hydride heat pump, an assessment of the potential applications and market sectors, a decision on the appropriate hydride alloys, a filter design study, development of transient heat transfer models and comparisons with experiments, and the design of an advanced hydride heat exchanger.

Phase II consisted of the experimental verification of the hydride alloy design data, fabrication of the hydride heat exchanger module components, heat transfer testing of a single heat exchanger element and preliminary performance testing of the entire module. This phase began in March 1982 and ended in December 1982. Phase III was devoted to the operation and testing of the hydride modules and a review of other hydride heat exchanger designs. Phase III began in November 1983 and was completed in July 1984.

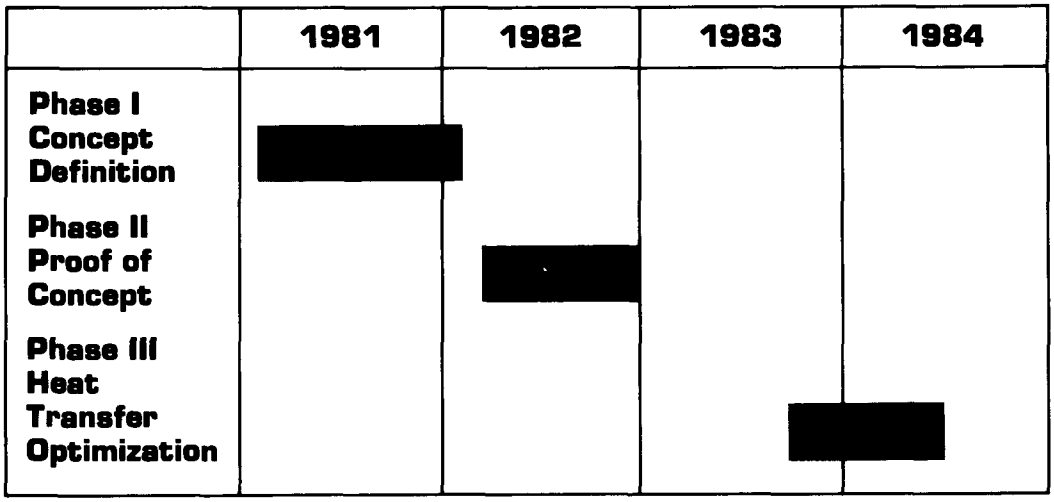

Figure 2. Project Schedule

2.3 FINAL REPORT ORGANIZATION

This final report is organized in the following manner:

- The Performance Testing section outlines the performance predictions and calculations, the test facility, the test objectives and testing results.

- The Design Review chapter focuses on the evaluation of the advanced hydride heat exchanger design and compares actual test data to the performance predictions.

- The section on Heat Transfer Concept Comparisons identifies and reviews other heat exchange concepts that improve heat transfer within hydride alloys.

- The final chapter, Conclusions and Recommendations, summarizes the Phase III results and outlines areas were further development work is warranted.

3

PERFORMANCE TESTING

3.1 PERFORMANCE ESTIMATES

Predictions on performance based upon the actual heat exchanger module and hydride alloy characteristics and dimensions were calculated. Estimates on packing factor, hydride utilization factor, sensible heat, thermal mass ratio, cycle time, capacity and Coefficient of Performance (COP) are included.

The relevant properties of the selected hydride alloys, $LaNi_5$ and $MmNi_{4.15}Fe_{0.85}$, used in the calculations are listed in Table 1 and Table 2 tabulates the characteristics of the finned copper tube heat exchanger.

3.1.1 Packing Factor

The process of hydrogen absorption and desorption causes the metal crystal lattice to expand and contract leading to the comminution of the original hydride alloy particles. After many such cycles, the process of comminution produces a progressively greater proportion of fine particles. In order to prevent rupture of the hydride containment vessel, 100 percent filling of all the void space with hydride powder does not occur. Instead a packing factor is utilized which allows room for expansion of the hydride particles. The optimum packing factor for this design is 50 percent.

The available volume per heat exchanger vessel for the hydride powder is calculated based on the available space between fins on the copper tube.

$$\text{Available Volume per Vessel for Hydride} = \left(\frac{\pi}{4}\right)\left(\text{Fin OD}^2 - \text{Tube OD}^2\right)\left(\text{Fin Spacing}\right)\left(\frac{\text{Fins}}{\text{Inch}}\right)\left(\text{Tube Length}\right)(\#\ \text{Tubes})$$

$$= \frac{\pi}{4}\left[(.75\ \text{in.})^2 - (.25\ \text{in.})^2\right](.125\ \text{in.})\left(\frac{7}{\text{in.}}\right)(12\ \text{in.})\ (14\ \text{tubes})$$

$$= 57.73\ \text{in}^3$$

$$\text{Maximum Weight of Hydride per Vessel} = \left(\text{Available Vol. per Vessel For Hydride}\right)\left(\text{Hydride Density}\right)$$

Table 1

Hydride Alloy Properties

Hydride Alloy Data	$LaNi_5$ Ref. 1)	$MmNi_{4.15}Fe_{0.85}$ (Ref. 2)
Mass Per Vessel - lbs	9.95	8.30
Density - lb/in^3	0.3	0.3
Specific Heat - Btu/lb°F	0.107	0.107
Thermal Conductivity - Btu/hr ft°F	0.43	0.43
Heat of Formation - Btu/lb	92.2	68.3

Table 2

Characteristics of the Finned Copper Tube Heat Exchanger

Copper Specific Heat	0.092 Btu/lb°F
Copper Density	0.323 lb/in^3
Copper Thermal Conductivity	200 Btu/hr ft°F
No. of Tubes Per Vessel	14
Tube Length	12 inches
Tube OD	0.25 inch
Tube ID	0.18 inch
Fin Thickness	0.0216 inch
Fin Height	0.25 inch
Fin Spacing	0.125 inch
Fins Per Inch	7

Table 7

Heat Pump Test Data Summary

Half-Cycle Time (Minutes)	Heat Input (Btu)	Net Refrigeration (Btu)	Half-Cycle Capacity (Btu/Min)	COP	Maximum Refrigeration ΔT (°F)
2	570	49	20	0.09	3.6
3	735	70	34	0.13	4.0
4	440	97	36	0.15	4.0
5	843	124	23	0.15	12.1
8	1306	231	28	0.18	5.6

$$= \quad (57.73\ in^3)\left(0.3\ \frac{lb}{in^3}\right)$$

$$= \quad 17.32\ lbs.$$

Actual weight and packing factor of hydride per vessel:

$$WSV = \frac{8.3\ lbs.\ (actual)}{17.32\ lbs.\ (maximum)} \longrightarrow 48\%\ Packing\ Factor$$

$$CSV = \frac{9.95\ lbs.\ (actual)}{17.32\ lbs.\ (maximum)} \longrightarrow 57\%\ Packing\ Factor$$

3.1.2 Hydride Utilization Factor

The input and output capacity of the hydride heat exchangers are a function of the heat of formation of the hydride alloys and the sensible heat of the components. The heat of formation is determined from the hydriding reaction across the flat plateau region of the characteristic isotherm for each alloy. The published values for the heat of formation for a given alloy assumes that the full plateau width is traversed. In actual operation, a small amount of the hydride will remain inactive (not absorbing hydrogen) and the full plateau width will not be utilized. Therefore, in computing the actual heat of formation of a hydride alloy, the theoretical value will be multiplied by a utilization factor derived from empirical results to adjust the heat of formation to a more realistic value. Based on previous development work with hydride alloys, the assumed hydride utilization factor is 75 percent (i.e. 25% of each hydride is assumed to be inactive).

3.1.3 Sensible Heat

Sensible heat refers to the burden for heating and cooling the heat exchanger components, containment structure and hydride powder. It is important to minimize this quantity because, when testing the heat exchangers in the heat pump mode, operation is as a cyclical device and the parasitic sensible heat losses reduce the net useful output energy. It is also important to correctly predict the sensible heat losses as capacity and COP predictions are based on this evaluation.

In the hydride heat exchanger design the component sensible heat values that can be calculated are for the hydride powder, the finned copper tubing, the copper u-tubes, the aft plate and the insulation surface contacting the hydride tube bundle.

In general:

Sensible Heat = (Component mass) (Specific Heat)

Table 3 lists the calculable sensible heat values. The sensible heat total for the WSV is 1.63 Btu/°F and 1.81 Btu/°F for the CSV. This estimate is considered to be low due to the indeterminate sensible heat losses to the filter, flange head, pressure vessel body and remaining insulation mass. These losses could only be determined through experimental testing.

3.1.4 Thermal Mass Ratio

The thermal mass ratio is an important parameter as it describes the ratio of the sensible heat of the hydride powder to the sensible heat of the entire structure including the hydride. The goal is to minimize the sensible heat of the structure and achieve maximum hydride usefulness. Therefore, the optimum value of the thermal mass ratio for a zero mass heat exchanger is one.

The estimated thermal mass ratios for the hydride heat exchangers are:

$$\text{WSV Thermal Mass Ratio} = \frac{SH_{LaNi_5}}{\text{Total SH}} = \frac{0.89 \text{ Btu/°F}}{1.63 \text{ Btu/°F}} = 0.55$$

$$\text{CSV Thermal Mass Ratio} = \frac{SH_{MmNi_{4.15}Fe_{0.85}}}{\text{Total SH}} = \frac{1.07 \text{ Btu/°F}}{1.81 \text{ Btu/°F}} = 0.59$$

3.1.5 Cycle Time

In order to minimize the quantity of metal hydride powder necessary per useful output, a reduction in cycle time and a minimizing of the parasitic thermal losses to the structure must be accomplished. However, a reduction in cycle time is most critical since the capacity of the hydride heat exchangers in the heat pump test mode is calculated by dividing the net energy output by the total cycle time, i.e. a reduction in cycle time increases the capacity.

The finned copper tube heat exchanger was designed for minimal cycle time. The computer modeling in Phase I (Ref. 4) indicated that the lowest cycle time that could be achieved with this design was 1.13 minutes. However, this estimate was based on a temperature change in the heat exchange structure due to constant heat generation and on an uncorrected value for the hydride heat of formation. Discrepancies exist between the computer model and actual circumstances, because, in reality, the heat is not uniformly generated. That is, as the hydrogen is absorbed or desorbed into the hydride, it generates or absorbs heat that raises or lowers the temperature of the surrounding material if it is not removed. This rise in temperature locally affects the ability of the surrounding hydride to absorb or desorb the hydrogen and to produce or absorb heat.

Table 3

Component Sensible Heat Values

Component	Mass (lbs)	Specific Heat (Btu/lb°F)	Sensible Heat (Btu/°F)	
			WSV	CSV
Hydride Powder:				
$LaNi_5$	8.3	0.107	0.89	---
$MmNi_{4.15}Fe_{0.85}$	9.95	0.107	---	1.07
Finned Copper Tubing	3.93	0.092	0.36	0.36
Copper U-tubes	0.29	0.092	0.03	0.03
SS Aft Plate*	2.00	0.120	0.24	0.24
SS Insulation Surface*	0.91	0.120	0.11	0.11
TOTAL SENSIBLE HEAT			1.63	1.81

*SS = Stainless Steel

Although the modeling took into account the sensible heat of the finned tubing and the hydride powder, it does not reflect sensible heat losses to the containment structure. Therefore, actual cycle times must include time to overcome these losses also. A total cycle time goal of four minutes was established for this design (corresponding to a two minute half-cycle time).

3.1.6 Capacity

The net useful output capacity of the heat exchanger modules in the heat pump test mode is in terms of refrigeration. It is a function of the cold side hydride heat of formation, the cold side hydride utilization factor, the sensible heat load and the half-cycle time.

$$\text{Net Output Capacity} = \frac{\left(\begin{matrix}\text{Cold side}\\ \text{hydride heat}\\ \text{formation}\end{matrix}\right)\left(\begin{matrix}\text{Cold side}\\ \text{utilization}\\ \text{factor}\end{matrix}\right)\left(\begin{matrix}\text{Mass}\\ \text{of hydride}\end{matrix}\right) - \left(\begin{matrix}\text{Cold Side}\\ \text{sensible}\\ \text{heat}\end{matrix}\right)(\Delta T)}{(\text{Half-Cycle Time})}$$

Table 4, column A outlines the potential refrigeration capacity in terms of half-cycle times.

3.1.7 Coefficient of Performance

The hydride heat exchangers were tested in the heat pump test mode. The method of evaluating the efficiency of a heat pump is to calculate the Coefficient of Performance (COP). The COP for the refrigeration heat pump operation is defined as:

$$\text{COP} = \frac{\text{Net Refrigeration}}{\text{Net Heat Input}}$$

The ideal maximum COP is a ratio of the two hydride heats of formation. This value is 0.74. However, this is unrealistic because the COP is also dependent upon hydride utilization factors and sensible heat losses. The COP estimate with the assumed value of 75% hydride utilization factor for both hydrides and the estimated values of sensible heat as shown in Table 3 is:

$$\text{COP} = \frac{\left(\begin{matrix}\text{cold side}\\ \text{heat of}\\ \text{formation}\end{matrix}\right)\left(\begin{matrix}\text{hydride}\\ \text{utilization}\\ \text{factor}\end{matrix}\right) - \left(\begin{matrix}\text{cold side}\\ \text{sensible}\\ \text{heat}\end{matrix}\right)(\Delta T)\left(\frac{1}{\text{mass of cold side hydride}}\right)}{\left(\begin{matrix}\text{warm side}\\ \text{heat of}\\ \text{formation}\end{matrix}\right)\left(\begin{matrix}\text{hydride}\\ \text{utilization}\\ \text{factor}\end{matrix}\right) + \left(\begin{matrix}\text{warm side}\\ \text{sensible}\\ \text{heat}\end{matrix}\right)(\Delta T)\left(\frac{1}{\text{mass of warm side hydride}}\right)}$$

Table 4

Potential Refrigeration Capacity in Terms of Half-Cycle Times

Half Time Time (Minutes)	A		B		C	
	Capacity with 75% Utilization Factors and Estimated Sensible Heat		Capacity with 75% Utilization Factors and Actual Sensible Heat		Capacity with Actual Utilization Factors and Actual Sensible Heat	
	Btu/Min	Tons	Btu/Min	Tons	Btu/Min	Tons
1	356	1.78	258	1.29	181	0.91
2	178	0.89	129	0.65	91	0.45
3	119	0.59	86	0.43	60	0.30
4	89	0.44	65	0.32	45	0.23
5	71	0.36	52	0.26	36	0.18
6	59	0.30	43	0.22	30	0.15
7	51	0.25	37	0.18	26	0.13
8	45	0.22	32	0.16	23	0.11

$$COP = \frac{\left(68.3 \frac{Btu}{lb}\right)(.75) + \left(1.81 \frac{Btu}{°F}\right)(125-40°F)\left(\frac{1}{9.95\ lbs}\right)}{\left(92.2 \frac{Btu}{lb}\right)(.75) + \left(1.63 \frac{Btu}{°F}\right)(200-80°F)\left(\frac{1}{8.3\ lbs}\right)}$$

COP = 0.39 (Estimate)

3.2 TEST FACILITY

3.2.1 General Description of the Hydride Heat Exchangers

The hydride heat exchanger module (Fig. 3) was designed for maximum heat transfer with a minimized thermal mass. The design consists of 14 finned copper tubes in a staggered tube bundle arrangement. The hydride powder is stored in the annular spacing between the fins. The heat transfer media, water, flows through the finned tubes.

The 14 finned copper tubes are divided evenly so that seven tubes function as water inlets and seven tubes are water outlets. The flow path through the inlet and outlet tubes are connected by brazing an unfinned copper U-tube to each inlet and outlet tube for a total of seven connections. At the other end, two manifold configurations connect each set of seven tubes to the appropriate flow path. The manifold and flange configuration is machined to form the head assembly. This makes the flanged head and the tube bundle

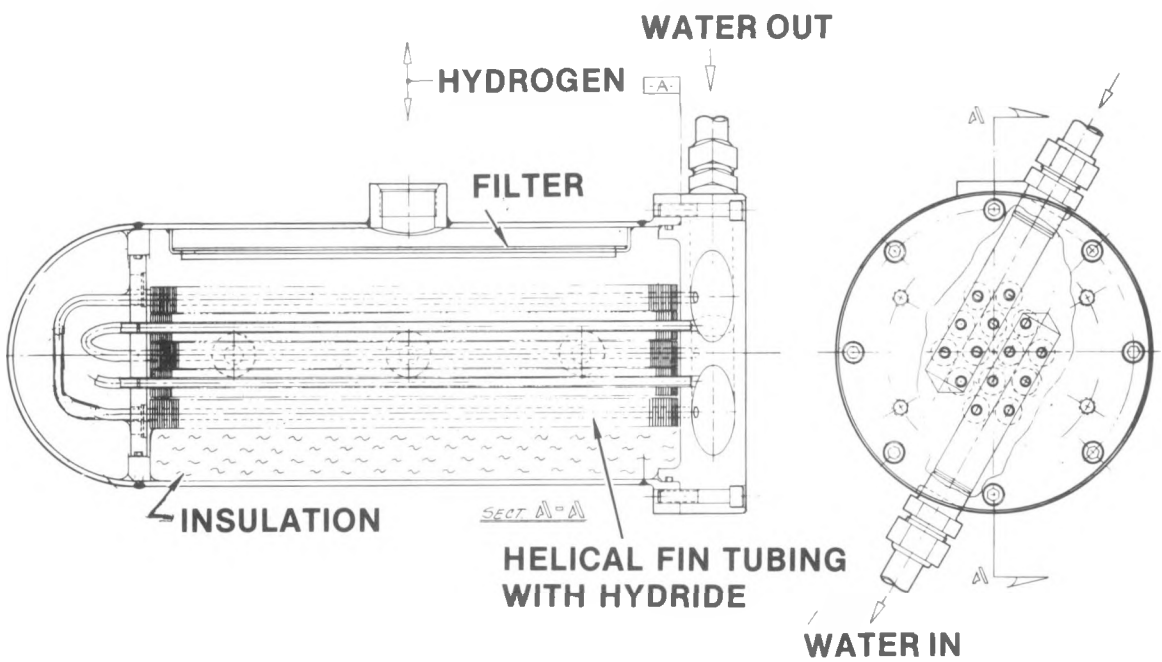

Figure 3. Hydride Heat Exchanger Schematic

arrangement integral components. This entire configuration is then loaded into a cylindrical pressure vessel.

The stainless steel vessel is a nominal 6.0 inch diameter pipe with a 0.25 inch wall thickness. It is designed with a hemispherical cap welded on at one end and with the flanged head assembly connected by eight bolts at the other. A radial separator is located at the hemispherical end of the vessel. Its purpose is to prevent the hydride powder from migrating from the finned tube section into the U-tube connections area. However, to prevent pressure buildup on one side of the separator, four "breathers" are machined into the 0.5 inch thick separator. These "breathers" are essentially filters that allow the hydrogen gas to circulate freely without pressure buildup and prevent hydride particle migration. The filter material is sintered stainless steel.

As well as functioning as "breathers", the filter material is also utilized in the hydrogen gas stream as the gas flows in and out of the pressure vessel. A filter is necessary so that the fine particles of the two hydrides do not intermix by traveling with the hydrogen gas. The filter in the heat exchanger module was designed with approximately 30 square inches of filter area which is sufficient to allow the hydrogen gas to rapidly escape with a low pressure drop. The filter is 10 inches long, 3 inches wide and 0.035 inch thick. It runs parallel to the tube bundle and is held in place by a stainless steel frame which is welded to the pressure vessel wall.

Insulation thermally isolates the finned tubes and the hydride particles from the high mass pressure vessel. The insulation units consist of a stainless steel outer skin with fiber insulation packed inside. There are two halves to each insulation unit to allow a close fit around the finned tube heat exchanger.

After the pressure vessel is fabricated and pressure checked, the hydride powder is loaded into the vessel through fill ports located on each side of the vessel. The ports are staggered along the vessel wall, three on one side and two on the other. This allows for equal and uniform filling of the hydride powder into the voids between the fins. There are also hydride fill ports in each half of the insulation units which match the corresponding fill ports in the pressure vessel wall.

The hydrogen flow path is located at the top of the horizontal vessel. The 0.75 inch OD hydrogen path is short and allows rapid hydrogen flow. For safety reasons, a relief valve, set to crack at 450 psig, is located in this line.

Figures 4 and 5 illustrate the mounted hydride heat exchanger modules and the refrigeration heat pump test facility.

3.2.2 Heat Pump Test Facility

The refrigeration heat pump test facility is located in Solar's Research Laboratories in San Diego, California. The test facility, as shown in the

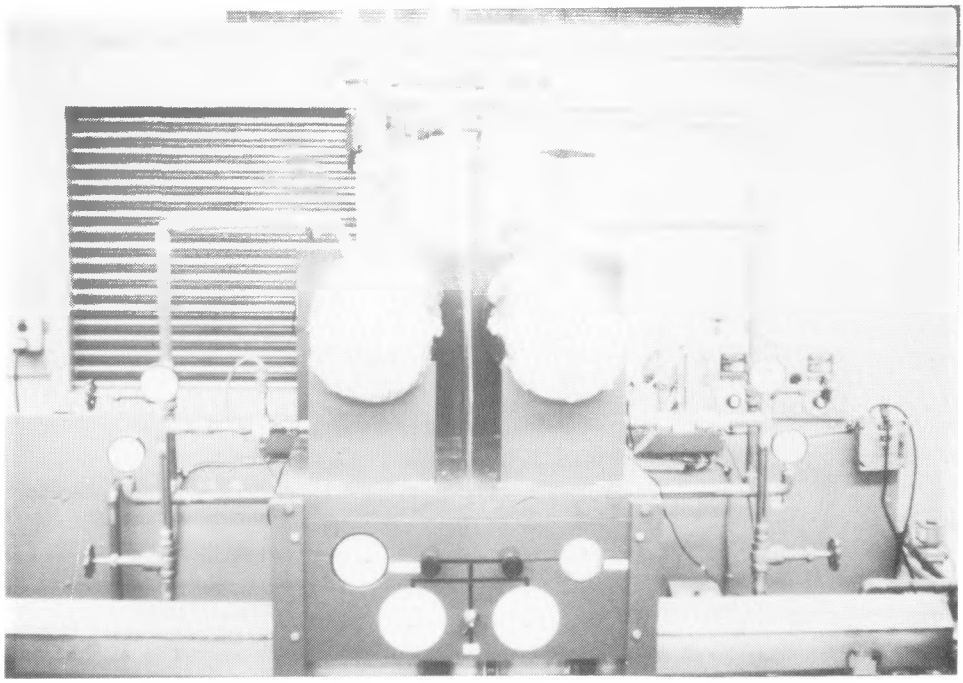

Figure 4. Hydride Heat Exchanger Vessel Mounted on Heat Pump Test Facility

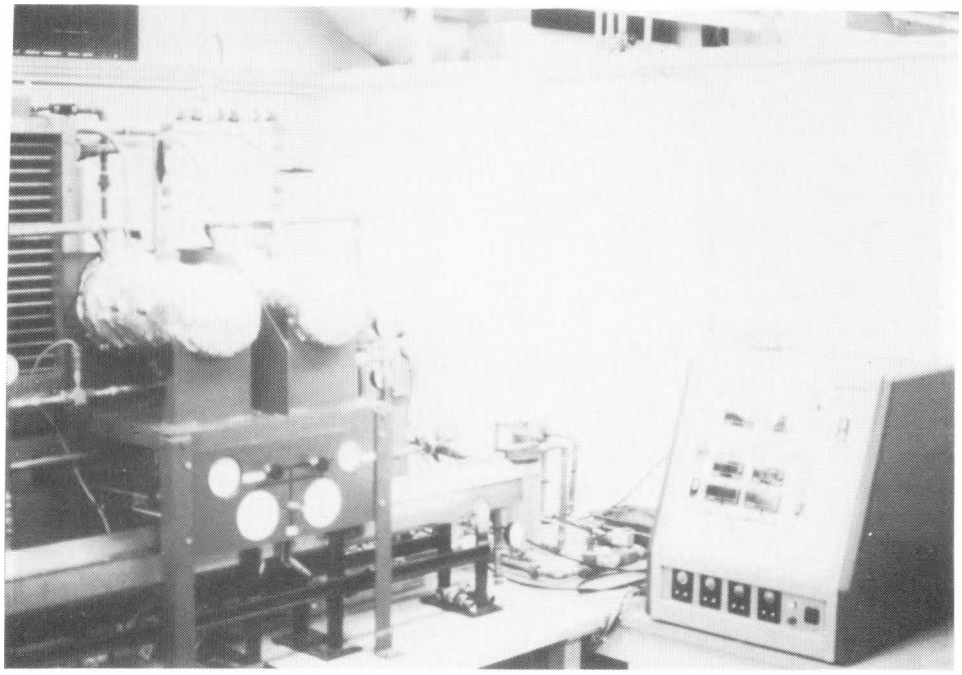

Figure 5. Refrigeration Heat Pump Test Facility

Figure 6 schematic, is controlled by a series of valving operations and three water flow paths -- cold, medium and hot water temperature loops.

The refrigeration system operates in the following manner. (CSA in Figure 6 refers to $MmNi_{4.15}Fe_{0.85}$ and WSA refers to $LaNi_5$.) Hot water at T_H is circulated through the WSA which allows the WSA to desorb hydrogen while absorbing heat from the water. The hydrogen-depleted CSA is exposed to the medium temperature (T_M) water loop which allows it to absorb the hydrogen (pressure of WSA > pressure of CSA). This is the charge half of the cycle.

In the refrigeration half of the cycle, the WSA is exposed to T_M which lowers the hydrogen pressure. Since the CSA is now at a higher pressure, the hydrogen flows from the CSA to the vessel containing the WSA. Desorption is an endothermic reaction causing the water flowing through the CSA vessel to decrease in temperature. This is the refrigeration effect.

The actual test facility contains, in the high temperature loop, an 8 kW water circulation heater and a hot water storage tank. The medium temperature loop utilizes a water recirculator (chiller) that provides a constant supply of cooling water at a desired temperature (range = 40 to 120°F). This loop also contains a water storage tank. The cold temperature loop consists of a cold air heat exchanger (fan) which is used to reject the refrigeration effect and a cold water storage tank. Each loop contains a water filter that prevents solid particles from fouling the turbine flow meters.

3.2.3 Data Acquisition System

To accurately record and edit the performance test data of the hydride heat exchangers, a Monitor Laboratories 9300 data logger coupled with a Kennedy 9800 digital magnetic tape transport was utilized (Fig. 7). This enabled all thermocouple readouts of the system to be recorded on magnetic tape every five seconds. The data was then input into an IBM 360/370 computer where checking occurred for any recording errors that might have materialized during data acquisition. The computer program then converted the recorded time of day to an elapsed time and arranged the thermocouple data into an array. Additional programs edited the data array, calculated inlet/exit water temperature differences and plotted the data.

3.3 HYDRIDE MATERIAL TESTING

3.3.1 Test Objective

In Phase II (Ref. 5), it was determined that the hydride alloy loaded into the cold side heat exchanger vessel did not possess the distinctions and characteristics attributed to it in published hydride literature. This is very important, because in a heat pump test mode, it is necessary for two hydrides to work in tandem and if one hydride malfunctions, the system will

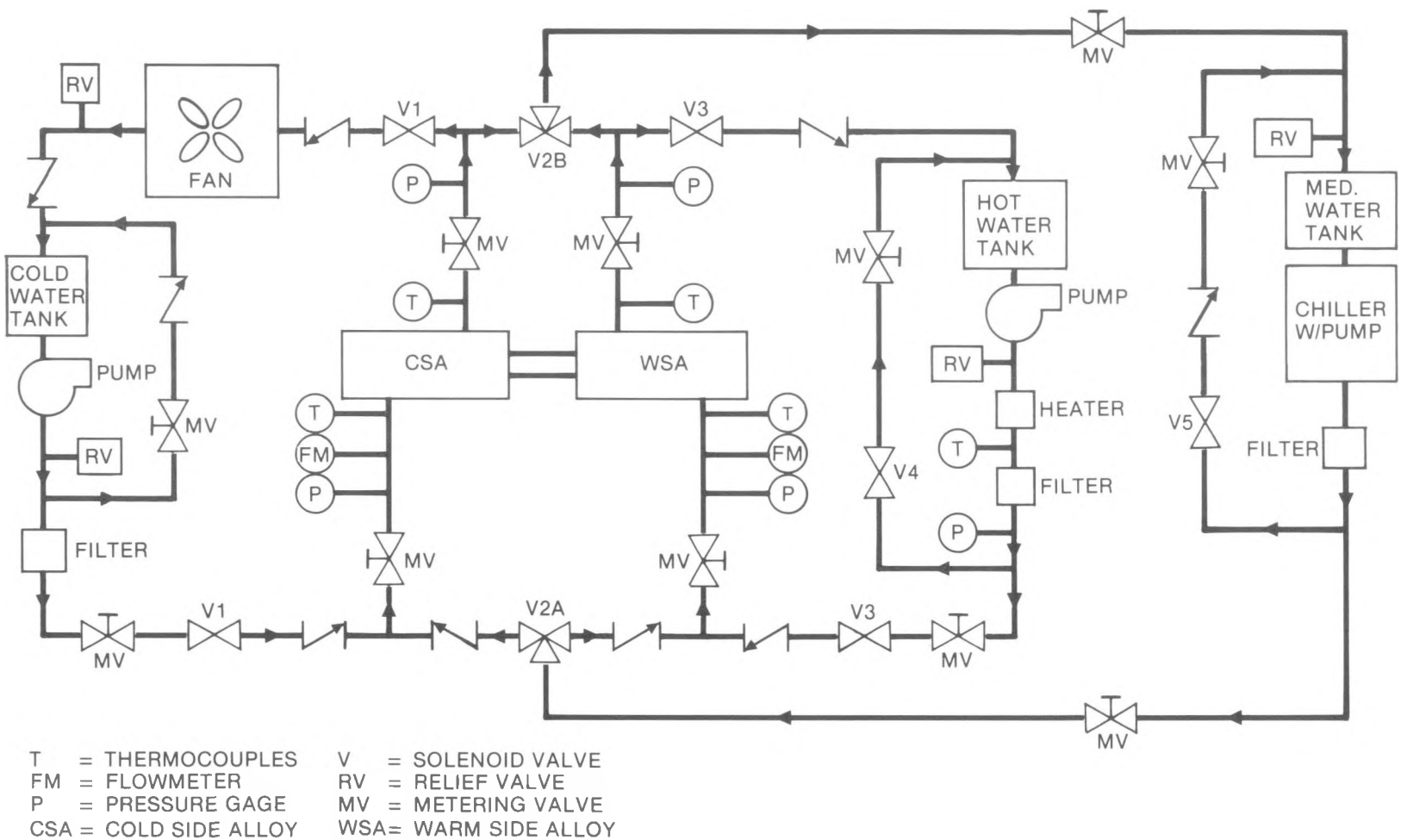

Figure 6. Schematic of Plumbing Operations of Test Facility

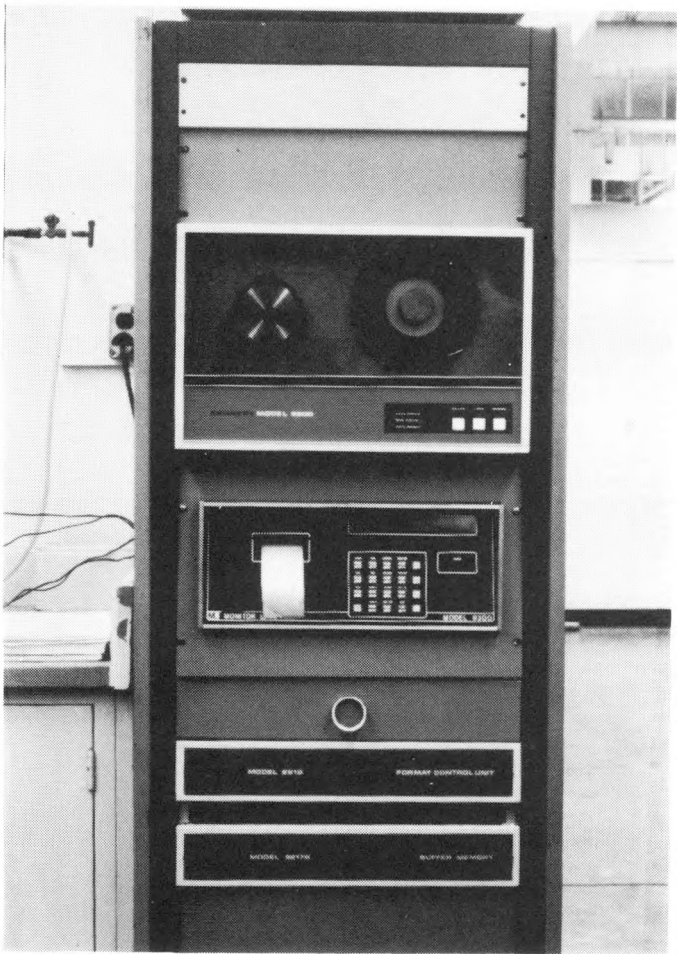

Figure 7.

Data Acquisition Systems

not operate. Therefore, in Phase III, the malfunctioning hydride alloy was replaced with a new batch of hydride.

Before loading of the new batch of $MmNi_{4.15}Fe_{0.85}$ into the CSV, the alloy was sent out to a local chemical analysis laboratory for metallographic examination. The results are shown in Table 5 and are compared to the alloy specifications as reported in the literature and to the previously - used batch of hydride alloy that was removed from the vessel. The new batch is slightly out-of-range compared to the specifications, however, this batch of alloy is part of a supply that has been used previously in a hydride heat pump mode at Solar and is known to operate correctly, so the decision was made to use this hydride alloy.

In addition, the new batch of hydride alloy was characterized by executing a desorption pressure composition isotherm at 45°F for further assurance of correct operation in a heat pump test mode.

Table 5

Chem Lab Analysis of $MmNi_{4.15}Fe_{0.85}$

Alloy Specifications (Refs. 6 and 7)		Lab Analysis of New Batch	Lab Analysis of Previously Used Batch
Ni	55.7	50.4	55.9
Fe	12.0	11.6	10.8
La	10.08 - 10.71	8.63	7.58
Ce	15.12 - 15.75	19.5	18.4
Nd	4.10 - 4.41	6.2	0.62
Pr	1.25 - 1.58	1.78	1.88
Other Rare Earths	0.32 - 0.63		

3.3.2 Test Results

The test apparatus used to generate the desorption pressure-composition isotherm is called the Hydride Characterization Test Rig and was described in Reference 5. The pressure - composition curve for $MmNi_{4.15}Fe_{0.85}$ at 45°F is shown in Figure 8. The mid-plateau pressure of approximately 5.7 atmospheres agrees with published hydride literature as well as matching the requirements as outlined in Reference 5. This data confirms that this batch of $MmNi_{4.15}Fe_{0.85}$ hydride alloy will operate successfully in the intended heat pump test mode.

3.4 SENSIBLE HEAT TESTING

3.4.1 Test Objective

Sensible heat testing of the hydride heat exchanger modules was important in order to determine the heat loss to all the components. The heat exchangers are to be characterized in the cyclical heat pump test mode and parasitic heating and cooling effects would tend to reduce the capacity and COP. Therefore, a goal of the design study was to minimize the sensible heat losses.

The sensible heat was estimated, as reported in Reference 5, based on the known mass of the system components and the specific heat (c_p) of those

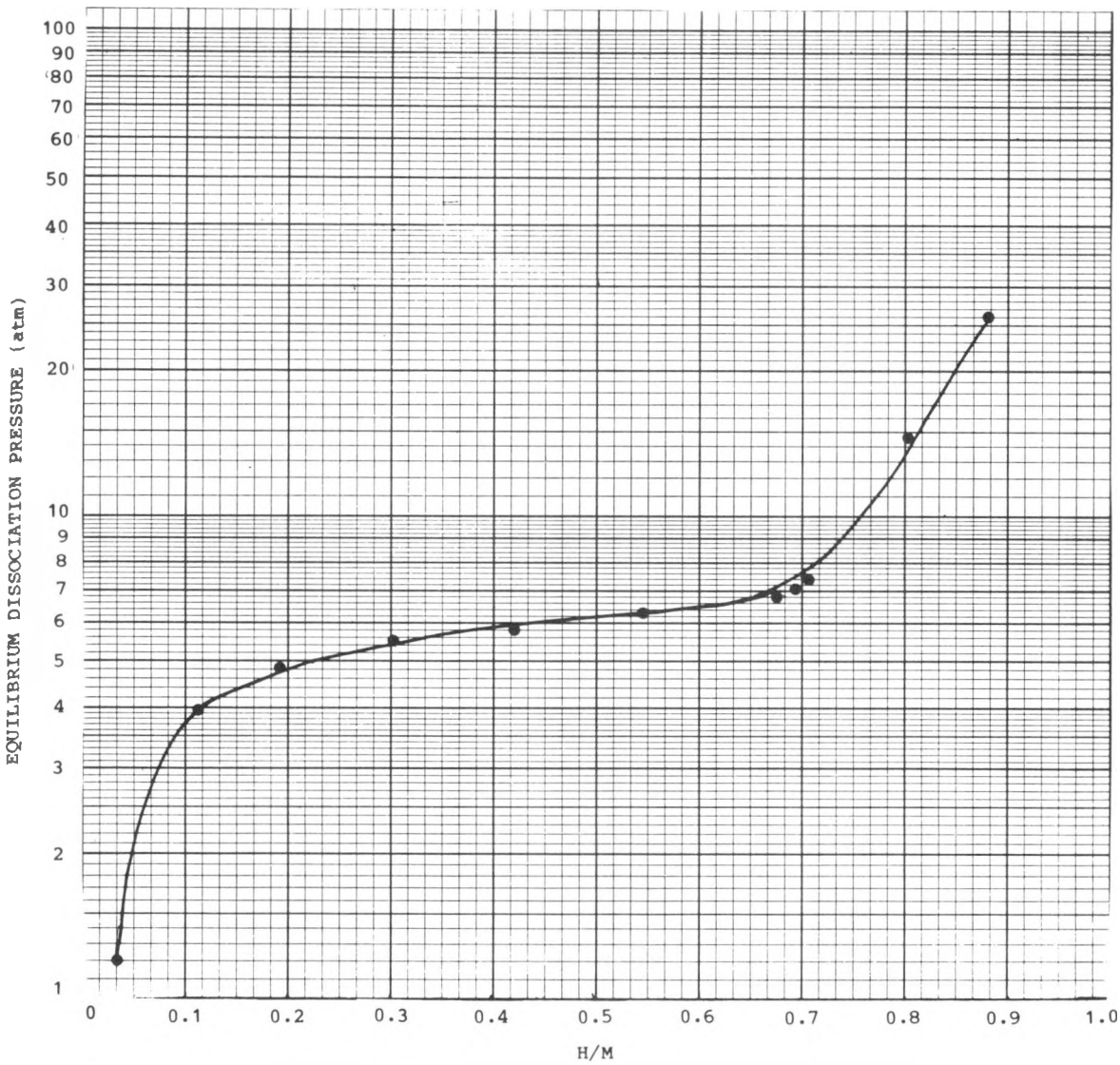

Figure 8. $MmNi_{4.15}Fe_{0.85}$ Pressure-Composition Isotherm

materials. The preliminary estimate was based only on the mass of the hydride powder and the copper finned tubes. This estimate was revised in Phase III to include the insulation surface contacting the hydride tube bundle and the aft plate. There are still sensible heat losses to the filter, flange head, pressure vessel body and remaining insulation mass that cannot be calculated. These losses could only be evaluated through experimental testing.

3.4.2 Test Results

In actual heat pump testing, each hydride heat exchanger will experience different temperature regimes. The CSV will range from 40°F to 125°F and the

WSV ranges from 80°F to 200°F. Therefore, sensible heat testing occurred at those ranges for each respective side.

Figures 9 and 10 are plots of the inlet and outlet water temperatures versus time for the warm and cold side, respectively. On each figure, the area between the two curves represents the total heat loss to the hydride heat exchanger components. These sensible heat quantities were calculated to be 2.367 Btu/°F for the WSV and 2.960 Btu/°F for the CSV.

The capacity and COP predictions are very dependent upon the sensible heat calculations. Therefore, since the actual sensible heat values are greater than the predictions (due to the incalcuable losses to the insulation, filter, flange head and pressure vessel body as outlined in Section 3.1.3), the capacity and COP were re-calculated for more accuracy in the predictions. At this point, the hydride utilization factors for both sides are still assumed to be 75%. Table 4, column B shows the re-calculated capacity; COP is shown below.

$$COP = \frac{\left(68.3 \frac{Btu}{lb}\right)(.75) - \left(2.960 \frac{Btu}{°F}\right)(125\text{-}40°F)\left(\frac{1}{9.95\ lbs}\right)}{\left(92.2 \frac{Btu}{lb}\right)(.75) + \left(2.367 \frac{Btu}{°F}\right)(200 - 80°F)\left(\frac{1}{8.3\ lbs}\right)}$$

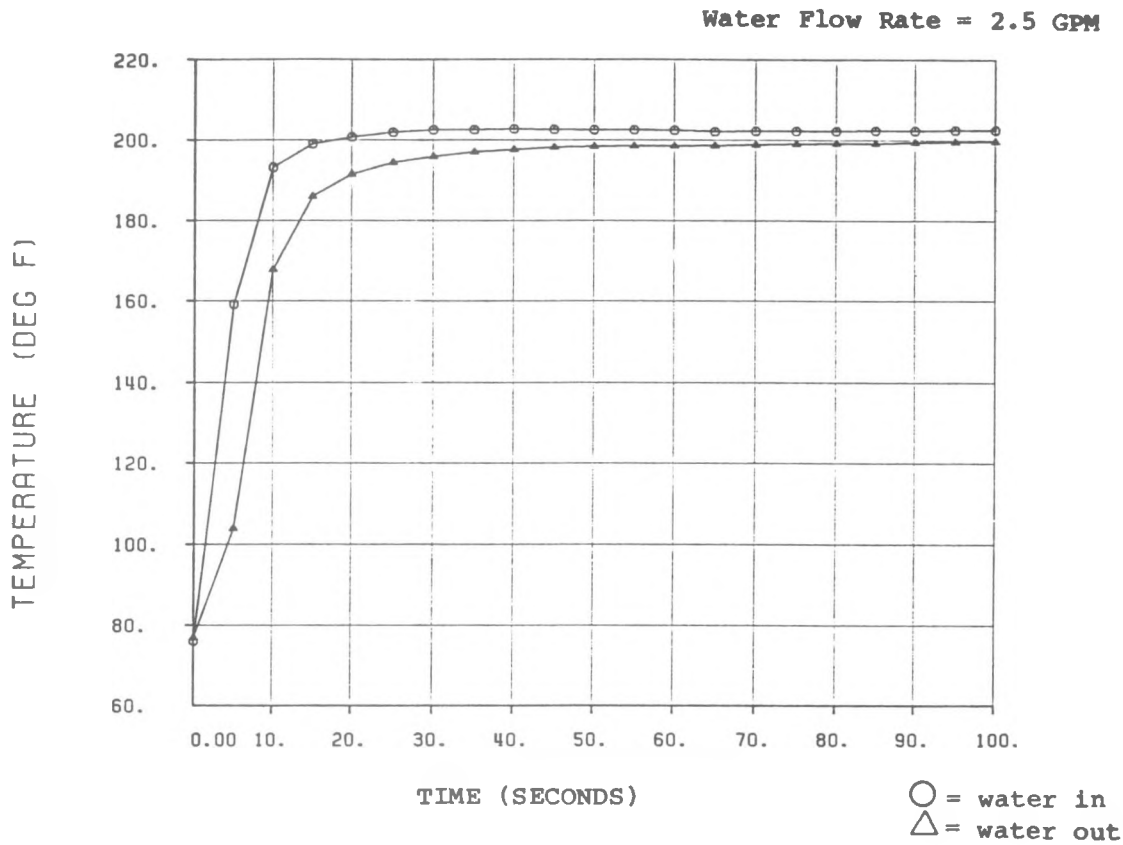

Figure 9. Sensible Heat Test - Warm Side Vessel

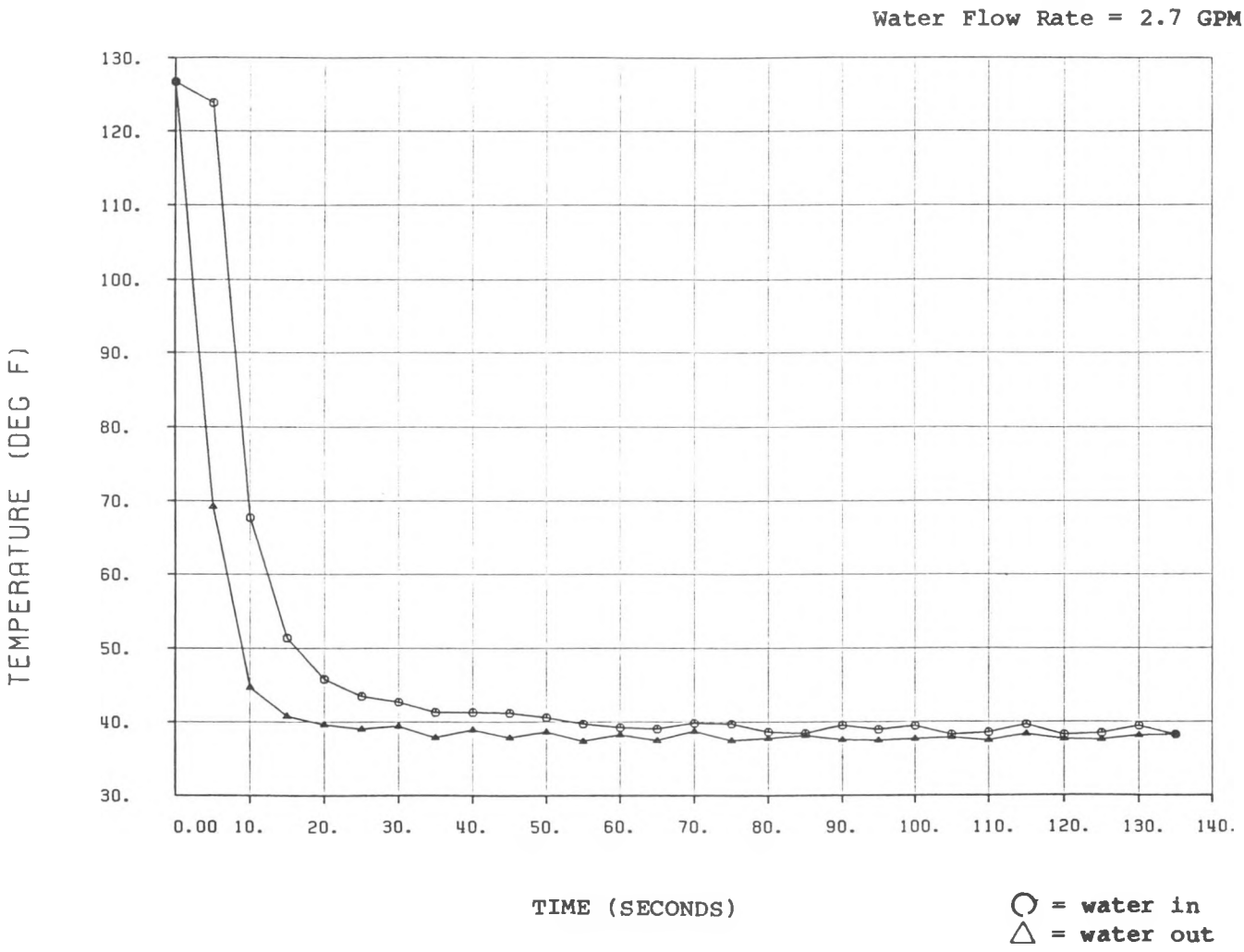

Figure 10. Sensible Heat Test - Cold Side Vessel

COP = 0.25

3.5 ISOLATION TESTING

3.5.1 Test Objective

Before actual cyclic heat pump testing occurred, each hydride module was isolated by a valve in the hydrogen flow path and individually pressurized with hydrogen or evacuated. From this test, the amount of active hydride in each vessel could be calculated resulting in an evaluation of the actual hydride utilization factor.

3.5.2 Test Results

Water at room temperature and 0.5 gpm flowed through each vessel during testing. The water temperature at the inlet and outlet to the heat exchangers was recorded. Hydrogen absorption produced an exothermic reaction; evacuation was endothermic. Figures 11 through 14 are plots of temperature vs. time for the warm side and the cold side vessels under hydrogen evacuation and pressurization. In each test, time was unrestricted; the inlet and outlet temperatures were allowed to come to equilibrium before the test was concluded.

The warm side vessel, containing $LaNi_5$, achieved a maximum water ΔT of -9°F (Fig. 11) during evacuation and a maximum of +30°F (Fig. 12) during hydrogen pressurization.

A similar test was conducted on the cold side vessel which contains the new batch of $MmNi_{4.15}Fe_{0.85}$. After evacuation, the subsequent decrease in water temperature reached a maximum of -11°F (Fig. 13) and hydrogen pressurization resulted in a ΔT of +8°F (Fig. 14). When compared to the isolation tests of the original batch of hydride alloy (Ref. 5) where pressurization resulted in only +2°F and evacuation in only -3°F, indications are that this new batch of $MmNi_{4.15}Fe_{0.85}$ is operating as expected.

These test results can also be used to calculate the actual hydride utilization factors. Figure 12 illustrates the heat output of the WSA upon hydrogen absorption. The area between the two curves represents the actual heat output and converts to 530.2 Btu. The estimated heat output is a function of the warm side heat of formation and the actual warm side sensible heat (which was evaluated in Section 3.4.2).

$$\text{WSV Estimated Heat} = \left[\left(\begin{matrix}\text{Warm Side}\\ \text{Heat of}\\ \text{Formation}\end{matrix}\right) - \left(\begin{matrix}\text{WSV Actual}\\ \text{Sensible}\\ \text{Heat}\end{matrix}\right)(\Delta T)\left(\frac{1}{\text{Mass of Hydride}}\right)\right]\left(\begin{matrix}\text{Mass of}\\ \text{Hydride}\end{matrix}\right)$$

$$Q_{est} = \left[\left(92.2\ \frac{\text{Btu}}{\text{lb}}\right) - \left(2.367\ \frac{\text{Btu}}{°\text{F}}\right)(30°\text{F})\left(\frac{1}{8.3\ \text{lbs}}\right)\right](8.3\ \text{lbs})$$

$$Q_{est} = 694.25\ \text{Btu}$$

$$\text{WSV Hydride Utilization Factor} = \frac{Q\ \text{Actual}}{Q\ \text{Estimated}} = \frac{530.2\ \text{Btu}}{694.25\ \text{Btu}} \longrightarrow 76.4\%$$

Similarily, Figure 13 illustrates the heat absorbed by the CSA upon hydrogen desorption. This calculates to 453.7 Btu. The estimated heat input is calculated by:

$$\text{CSV Estimated Heat} = \left[\left(\begin{matrix}\text{Cold Side}\\ \text{Heat of}\\ \text{Formation}\end{matrix}\right) + \left(\begin{matrix}\text{CSV Actual}\\ \text{Sensible}\\ \text{Heat}\end{matrix}\right)(\Delta T)\left(\frac{1}{\text{Mass of Hydride}}\right)\right]\left(\begin{matrix}\text{Mass of}\\ \text{Hydride}\end{matrix}\right)$$

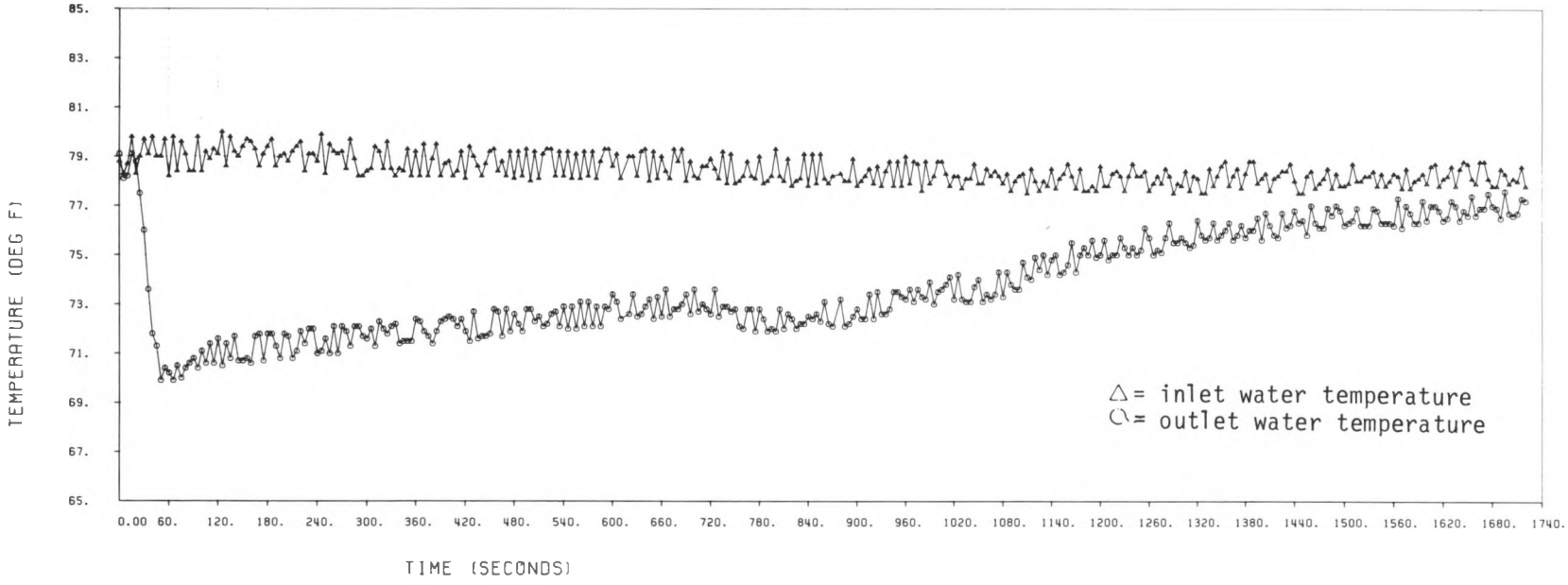

Figure 11. Warm Side Vessel Isolation Testing - Evacuation

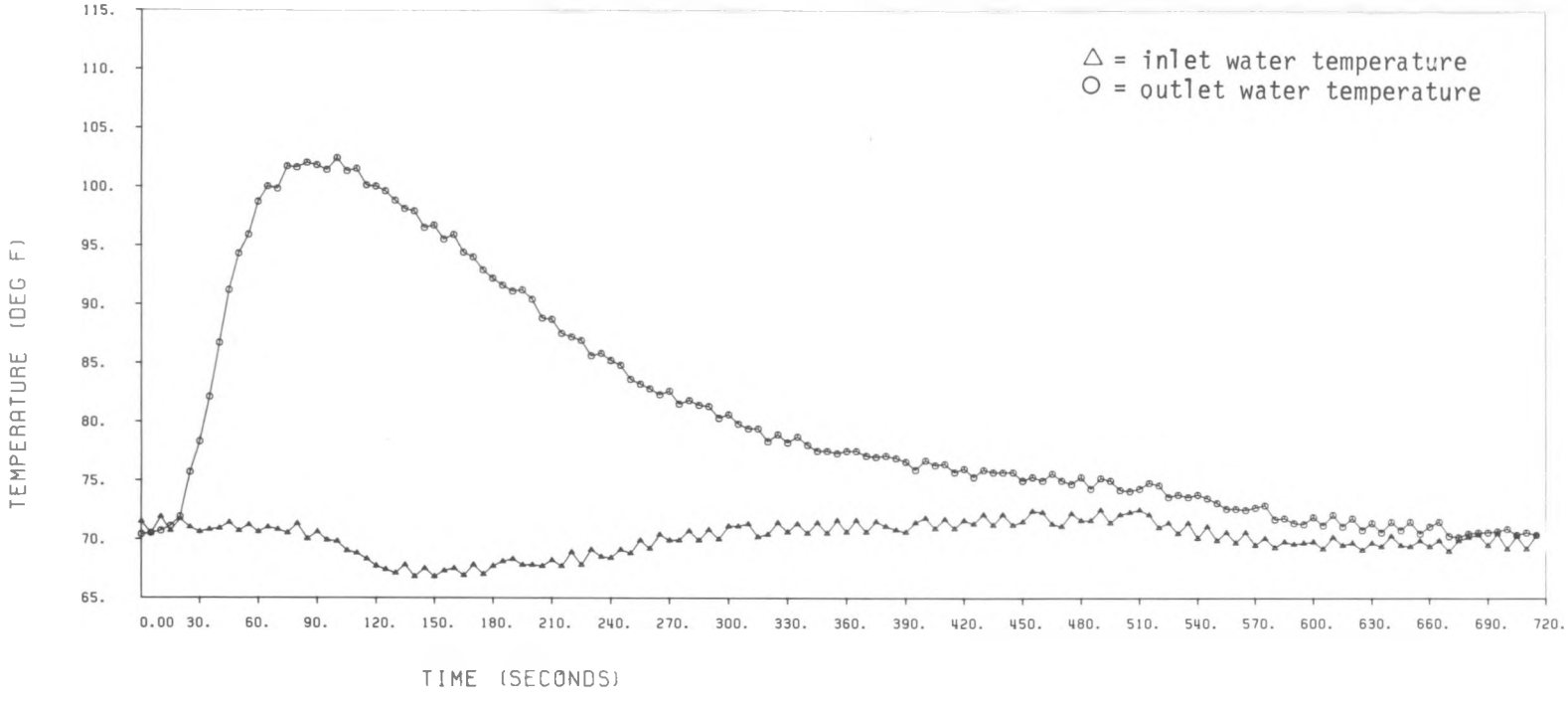

Figure 12. Warm Side Vessel Isolation Testing - Pressurization

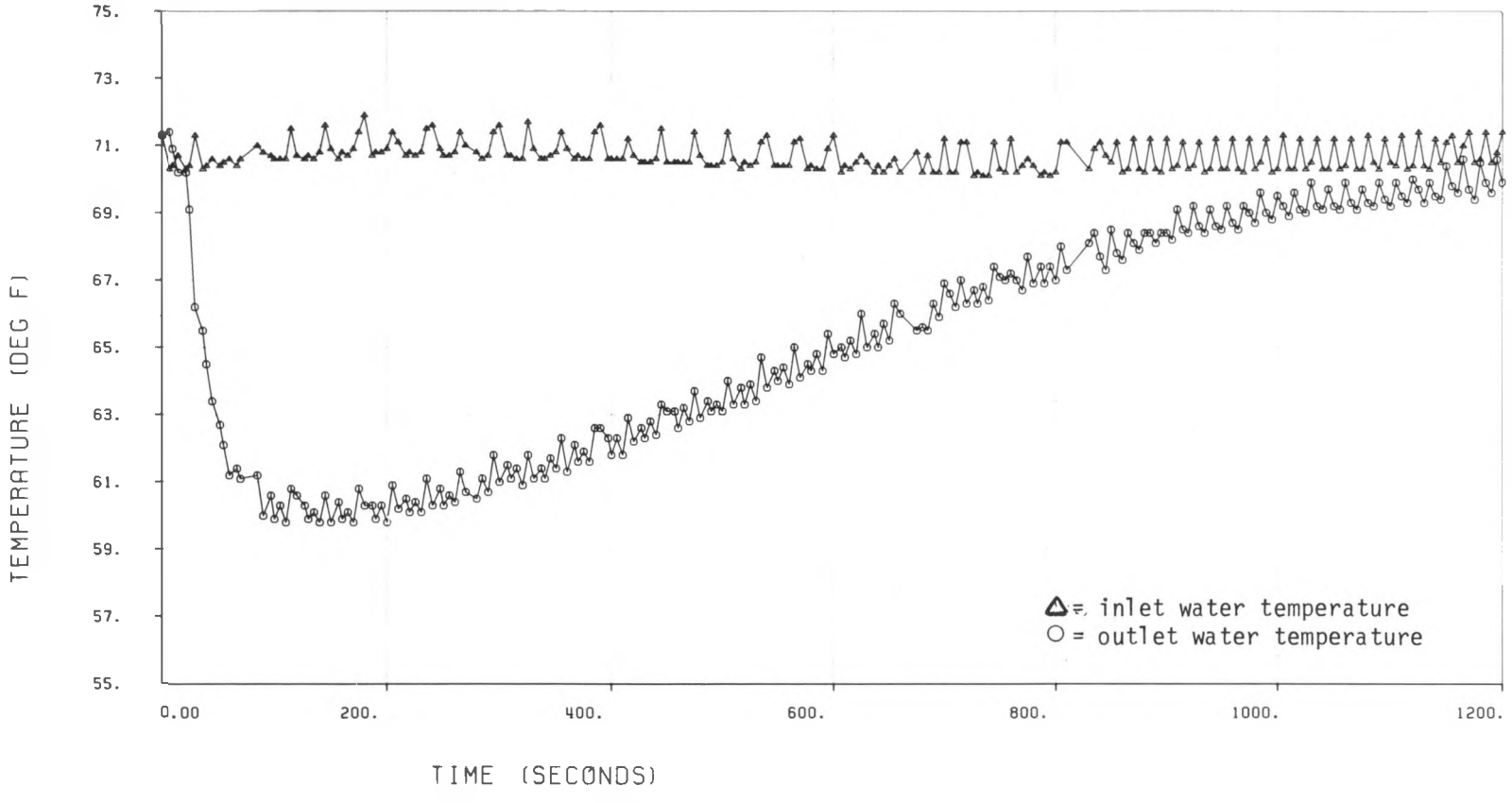

Figure 13. Cold Side Vessel Isolation Testing - Evacuation

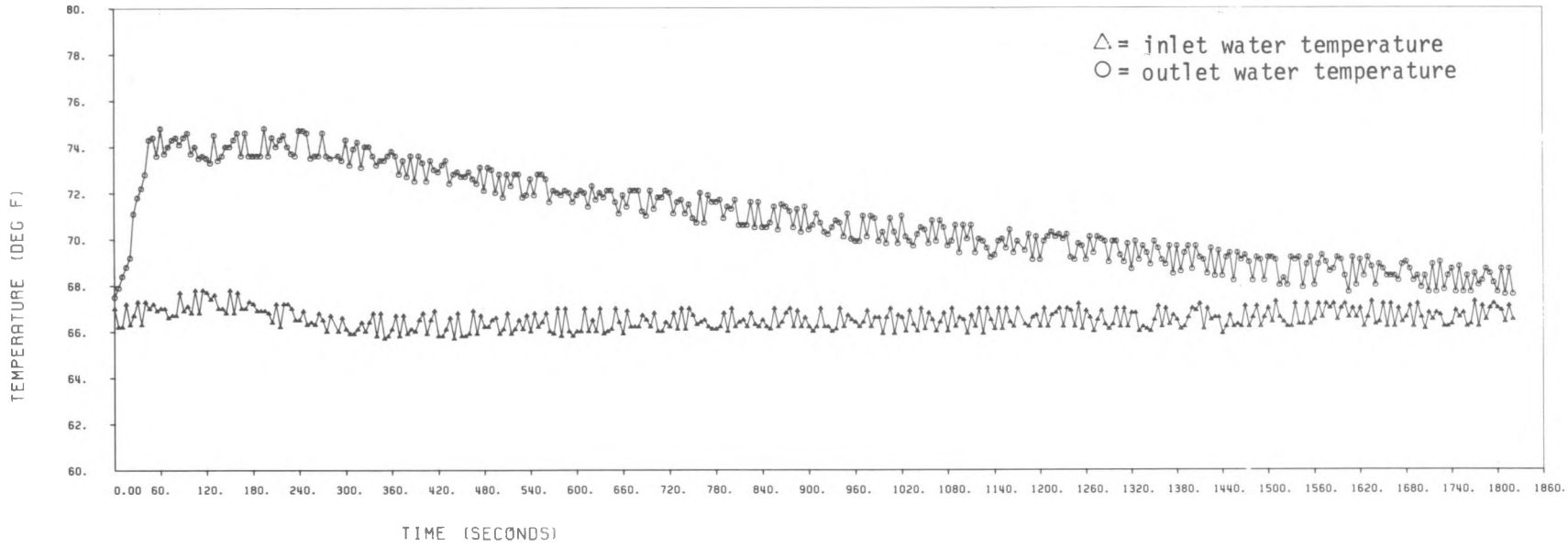

Figure 14. Cold Side Vessel Isolation Testing - Pressurization

$$Q_{est} = \left[\left(68.3 \frac{Btu}{lb}\right) + \left(2.96 \frac{Btu}{°F}\right)(11°F)\left(\frac{1}{9.95\ lbs}\right)\right](9.95\ lbs)$$

$$Q_{est} = 712.15\ Btu$$

$$\text{CSV Hydride Utilization Factor} = \frac{Q\ Actual}{Q\ Estimated} = \frac{453.7\ Btu}{712.15\ Btu} \longrightarrow 63.7\%$$

Recalculation of the capacity and COP values are again required based on the actual values of the hydride utilization factors. Capacity is shown in Table 4, Column C; COP is shown below.

$$COP = \frac{\left(68.3 \frac{Btu}{lb}\right)(.637) - \left(2.960 \frac{Btu}{°F}\right)(125 - 40°F)\left(\frac{1}{9.95\ lbs}\right)}{\left(92.2 \frac{Btu}{lb}\right)(.764) + \left(2.367 \frac{Btu}{°F}\right)(200 - 80°)\left(\frac{1}{8.3\ lbs}\right)}$$

$$COP = 0.17$$

3.6 HEAT PUMP MODE TESTING

3.6.1 Test objective

The project goal is the design, development and demonstration of a metal hydride heat exchanger/containment device. Testing this design in the refrigeration heat pump mode produced data on cycle time, capacity and Coefficient of Performance.

3.6.2 Test Results

The operational cycle of a hydride heat pump involves a charge phase and a refrigeration phase (Fig. 15). The charge phase encompasses the time period when the warm side alloy ($LaNi_5$) is heated from the intermediate temperature (T_M) to the firing temperature (T_H) and discharges hydrogen. The heat input during this phase consists of the heat required to fire the heat pump and is represented by the area between the warm side inlet and the warm side outlet curves. The refrigeration phase of the cycle encompasses the time period when the warm side alloy is cooled from the firing temperature (T_H) to the intermediate temperature (T_M) and the cold side alloy ($MmNi_{4.15}Fe_{0.85}$) discharges hydrogen. During the refrigeration phase, the cold side alloy is cooled from the intermediate temperature (T_M) to the low temperature (T_L) by the incoming water. The refrigeration produced is represented by the area between the cold side inlet and the cold side outlet curves.

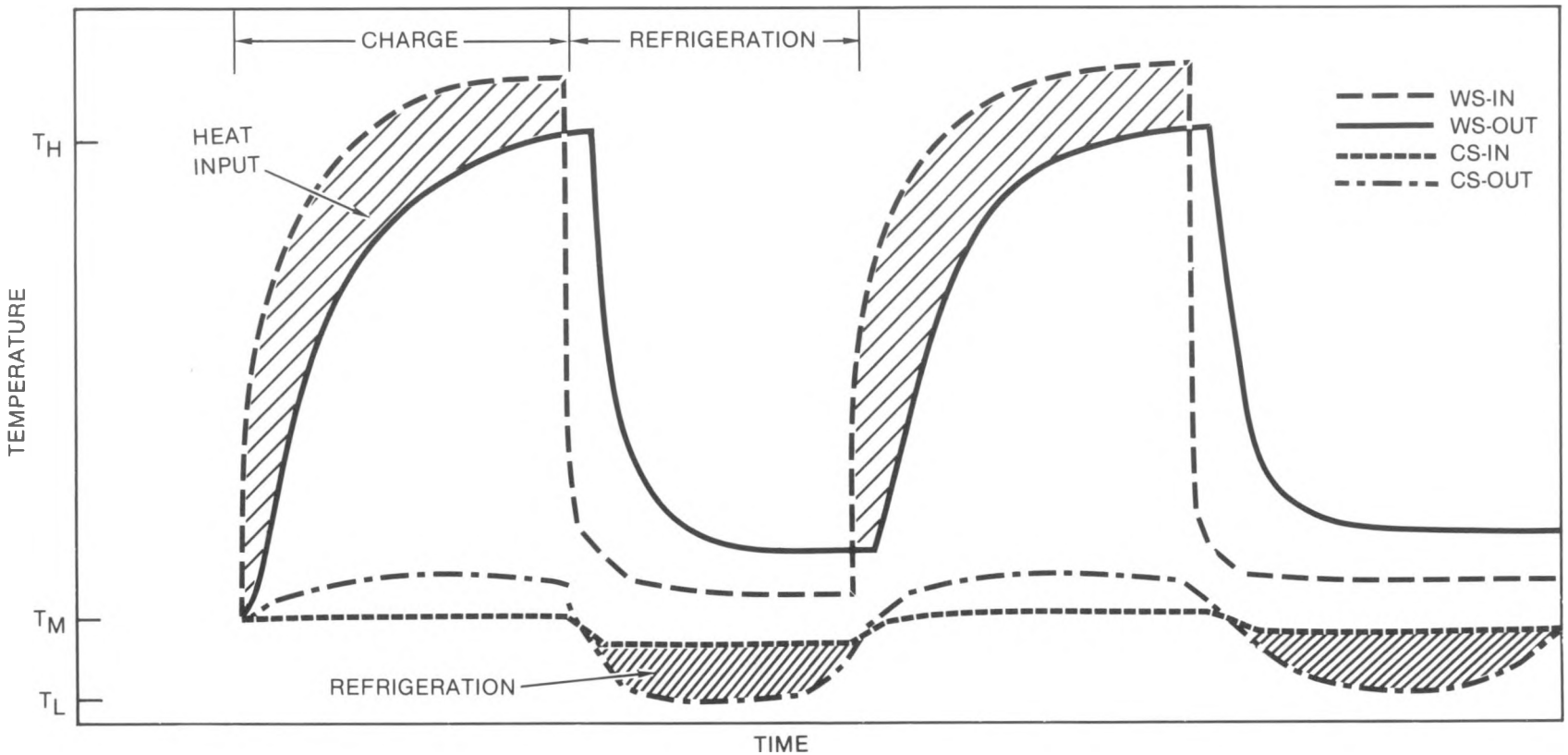

Figure 15. Typical Cycle for a Hydride Heat Pump Test

The recorded test data consisted of the warm side inlet and outlet water temperatures (°F), the cold side inlet and outlet water temperatures (°F), the warm and cold side water flow rates (gallons per minute) and the elapsed time.

In analyzing the accumulated data, the inlet and outlet water temperatures for the warm and cold sides were converted to total heat (Btu) absorbed or desorbed during the charge or refrigeration phase of the cycle. This total heat is determined by:

$$Q = \dot{m} \; C_p \; \Delta T$$

where

Q = total heat, Btu
$\dot{m}$ = water flow rate, gpm
C_p = specific heat, Btu/lb°F
ΔT = (outlet temperature - inlet temperature), °F

The capacity of the heat pump test mode is determined by dividing the net refrigeration produced by the total cycle time. The half cycle capacity is determined by dividing the net refrigeration produced by the elapsed time over which refrigeration was produced.

$$\text{Capacity} = \frac{\text{Net Refrigeration (Btu)}}{\text{Total Cycle Time (Min)}}$$

$$\text{Half Cycle Capacity} = \frac{\text{Net Refrigeration (Btu)}}{\text{Refrigeration Time (Min)}}$$

The Coefficient of Performance (COP) is defined as the net refrigeration divided by the heat input required to fire the heat pump.

$$\text{COP} = \frac{\text{Net Refrigeration (Btu)}}{\text{Heat Input at } T_H \text{ (Btu)}}$$

In an actual heat pump where the application is air conditioning/refrigeration, the inlet return water to the refrigeration side of the heat pump would be at a temperature of approximately 55°F and the required outlet temperature would be 45°F resulting in a cooling ΔT of 10°F. This temperature differential of 10°F is what the test rig should simulate. Since it is not possible to prechill the water in the cold loop, the inlet to the cold side was always approximately 75°F with the desired output at 65°F.

The first round of heat pump testing was with a five minute half-cycle time, constant warm side water flow rates during both charge and refrigeration phases, constant cold side water flow rate during the charge phase and a variable cold side water flow rate during the refrigeration phase. The refrigeration phase cold side water flow rate was varied from 0.25 to 1.25 gpm. Graphical results are presented in Figure 16 with tabular results in Table 6.

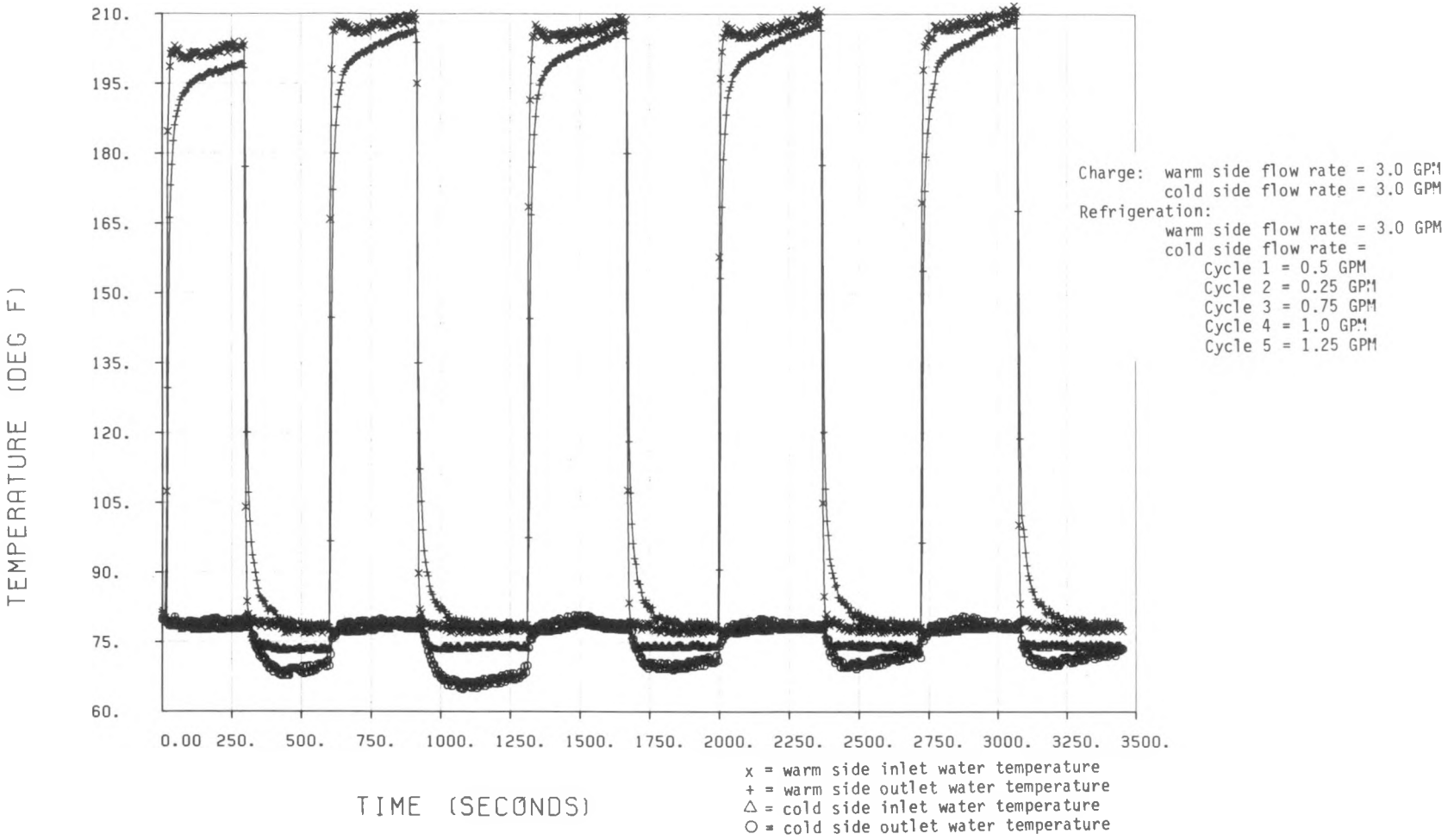

Figure 16. Heat Pump Test Mode, Half-Cycle Time = 5 Minutes, Cold Side Water Flow Rate Variations During Refrigeration

Table 6

Results of Cold Side Water Flow Rate Variations at
a Five Minute Half-Cycle Time

Cycle Number	Refrigeration Phase Cold Side Water Flow Rate (G.P.M.)	Heat Input (Btu)	Net Refrigeration (Btu)	Half-Cycle Capacity (Btu/Min)	COP	Maximum Refrigeration ΔT (°F)
1	0.5	1630	96	19.2	0.06	5.7
2	0.25	1121	82	12.4	0.07	8.9
3	0.75	1133	110	20.2	0.10	5.2
4	1.00	1048	137	23.4	0.13	4.9
5	1.25	1073	155	24.6	0.14	4.5

From this data, it is evident that capacity and COP increase with increasing cold side water flow rate, but the maximum refrigeration ΔT decreases.

The remaining series of tests were run at various half-cycle times, i.e. 2, 3, 4, 5 and 8 minutes and are presented in Figures 17 through 21. Various combinations of water flow rates were used, but this is only of concern when evaluating maximum refrigeration ΔT as was evident from Table 6.

The test data from this series of tests is presented in Table 7 and is discussed in the next section.

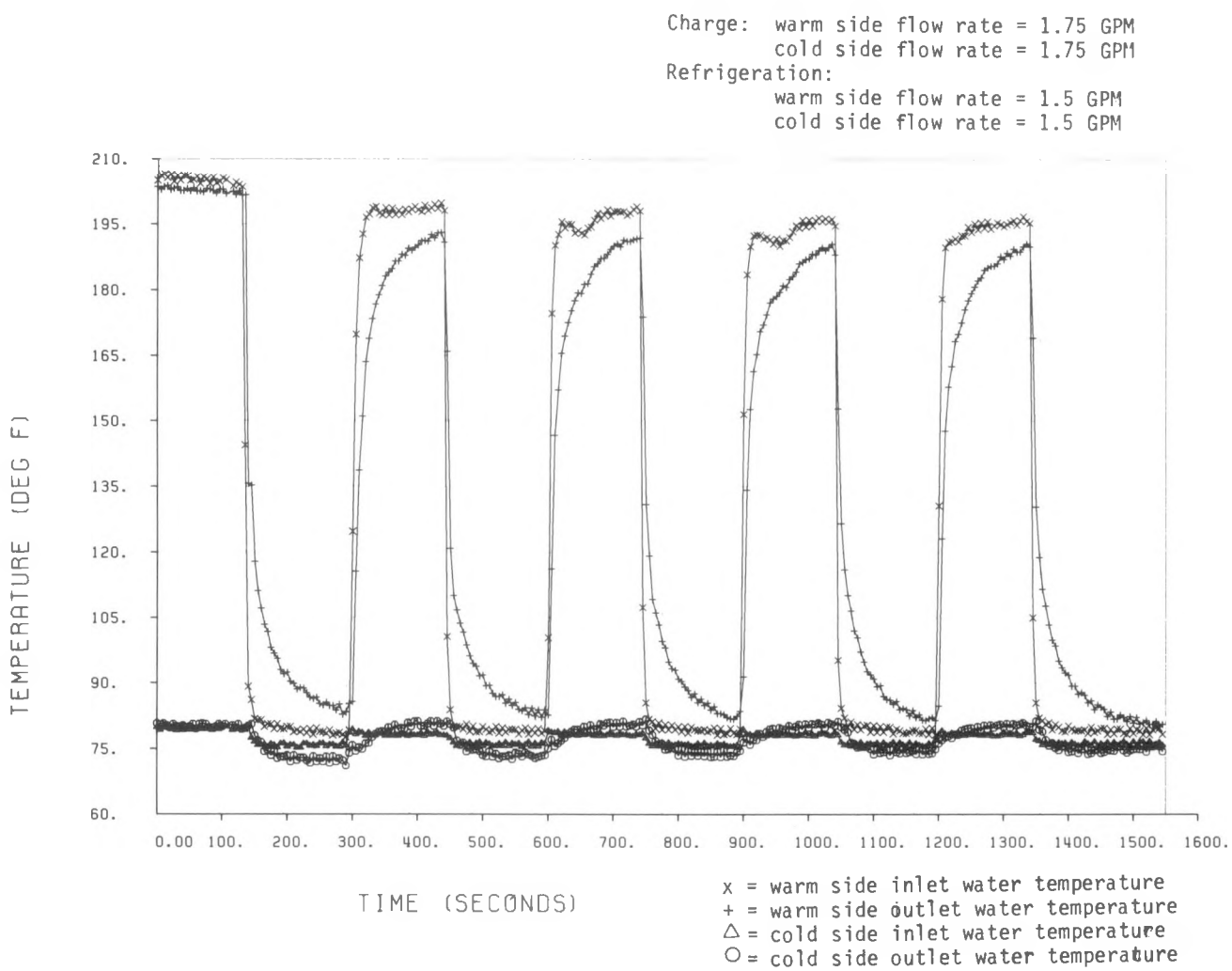

Figure 17. Heat Pump Test Mode, Half-Cycle Time $\cong$ 2 Minutes

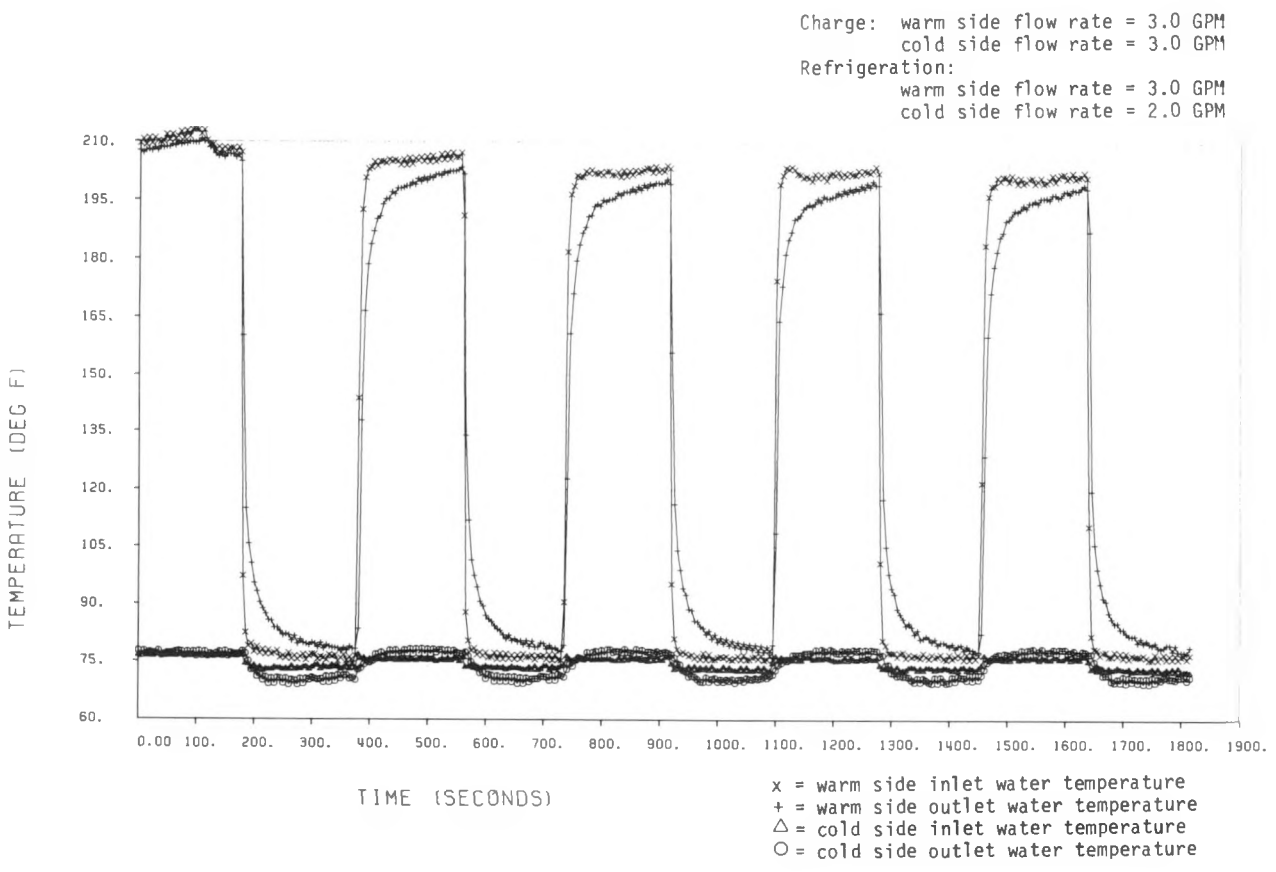

Figure 18. Heat Pump Test Mode, Half-Cycle Time ≅ 3 Minutes

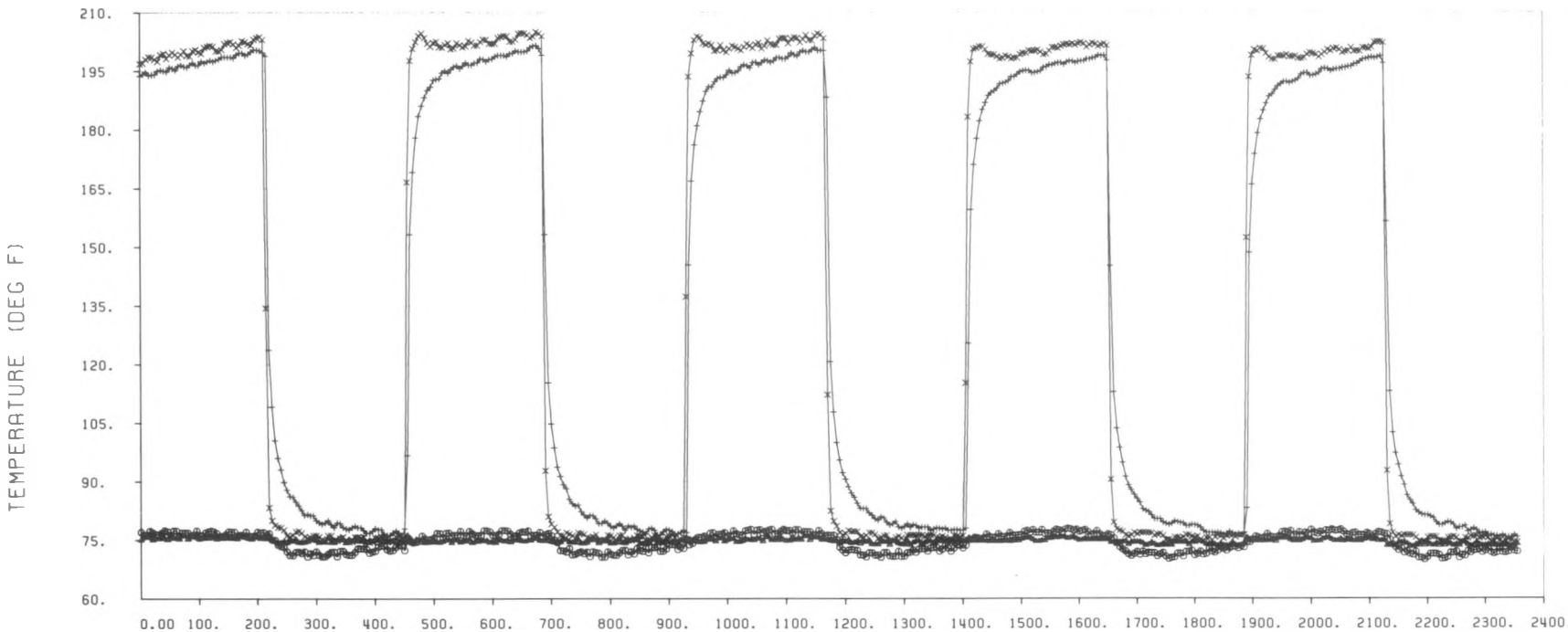

Charge: warm side flow rate = 3.0 GPM
cold side flow rate = 3.0 GPM
Refrigeration:
warm side flow rate = 3.0 GPM
cold side flow rate = 2.0 GPM

Figure 19. Heat Pump Test Mode, Half-Cycle Time = 4 Minutes

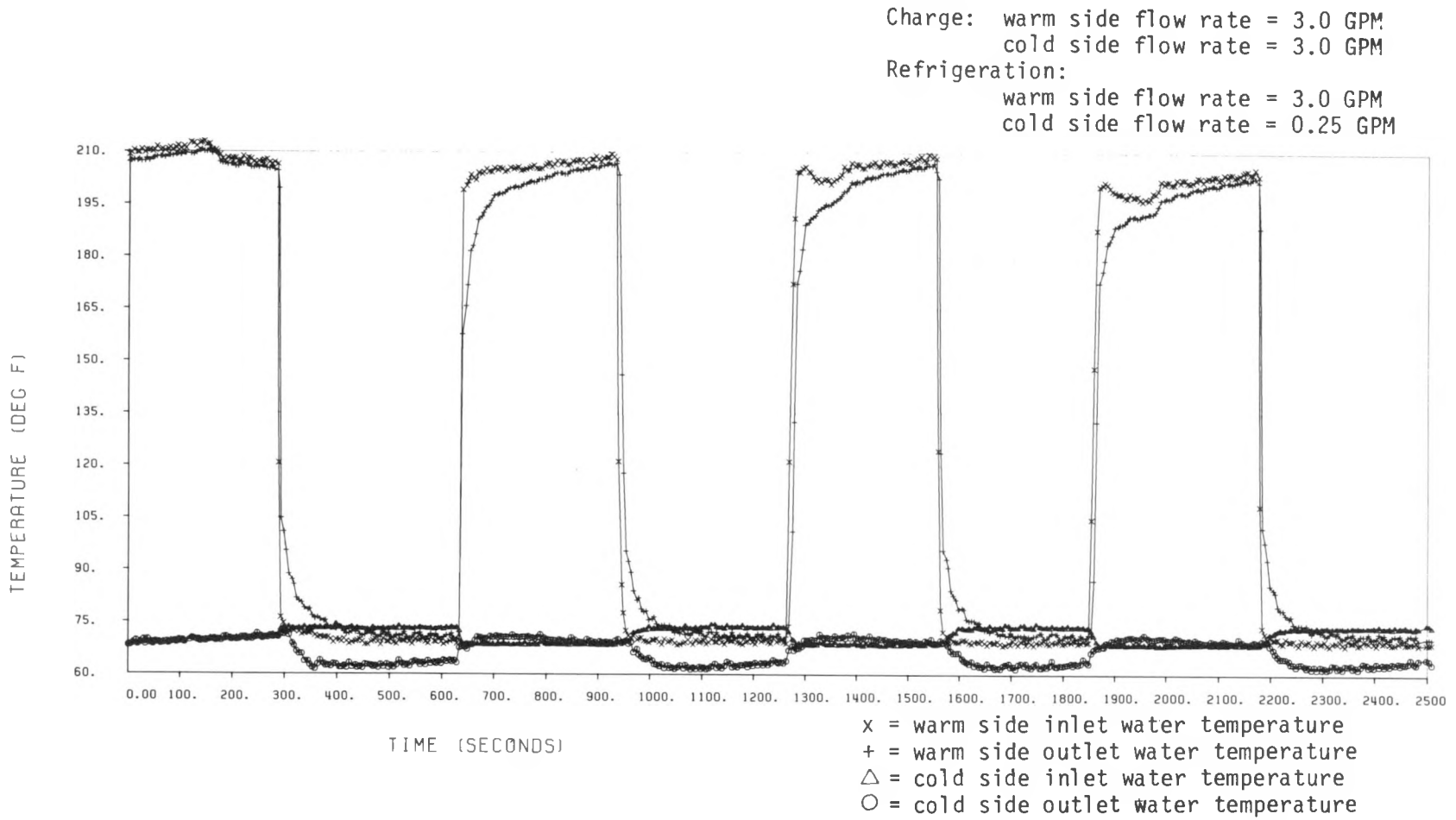

Figure 20. Heat Pump Test Mode, Half-Cycle Time = 5 Minutes

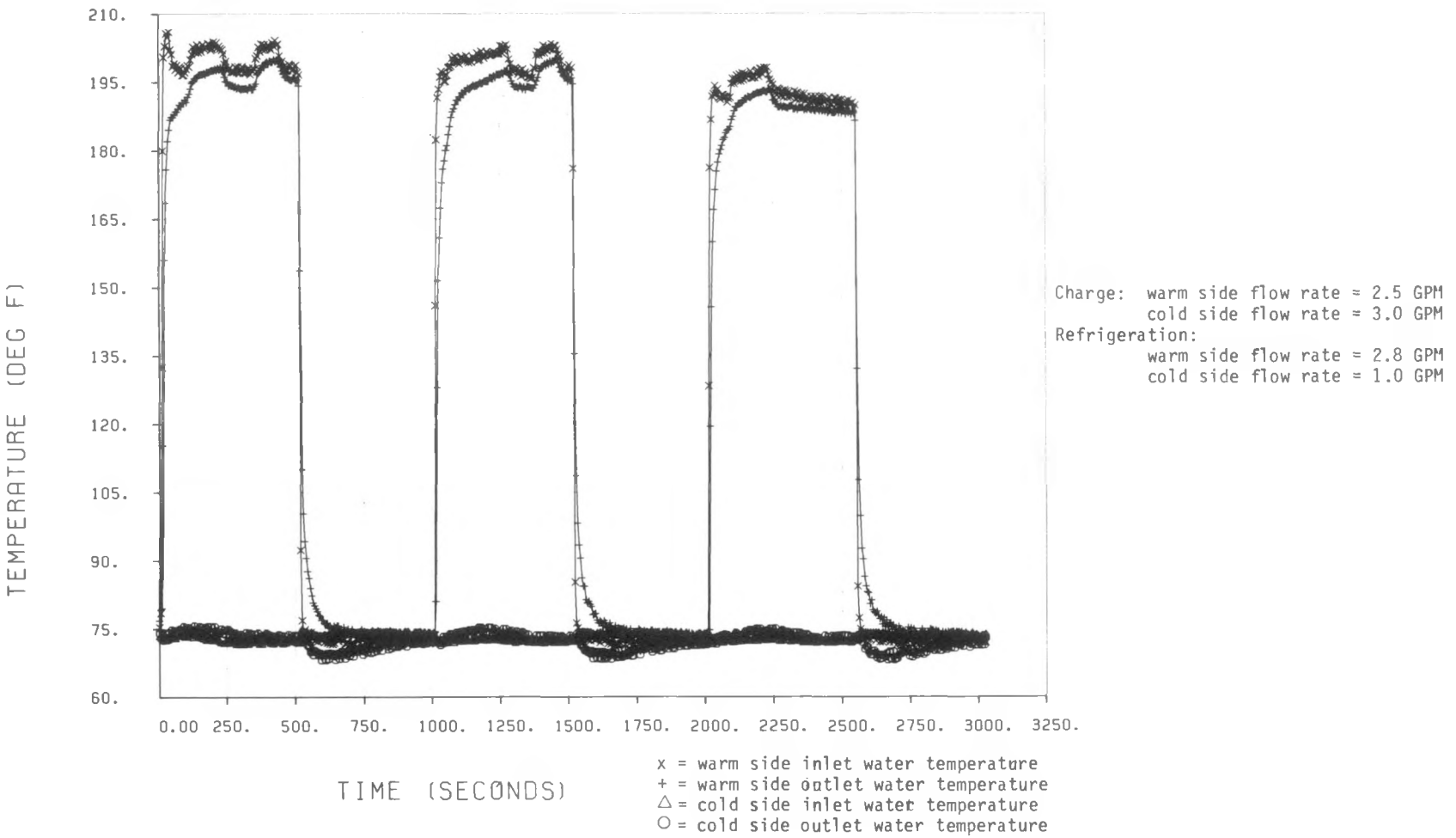

Figure 21. Heat Pump Test Mode, Half-Cycle Time ≅ 8 Minutes

4

DESIGN REVIEW

In reviewing the design of the hydride heat exchanger/containment device, performance predictions and actual data were compared.

4.1 PACKING FACTOR

A packing factor of 50% was the design choice for both hydride heat exchanger vessels. This is necessary to allow the hydride powder room to expand and to prevent rupture due to large internal pressure. The actual packing factors were 48% for the WSV and 57% for the CSV. The explanation for the range between the two vessels is that the amount of each alloy must be matched so that the working amount of hydrogen to be exchanged was identical for both sides. This results in different amounts of each alloy, since each alloy absorbs/desorbs a different amount of hydrogen gas. The actual packing factors are close enough to the 50% estimate, however, to forestall any concern of rupture.

4.2 HYDRIDE UTILIZATION FACTOR

For initial calculation purposes, the assumed hydride utilization factors for both hydride alloys was 75%. In Phase II, with the original batch of each hydride, the utilization factors were experimentally measured and resulted in a value of 72% for $LaNi_5$ and only 19% for $MmNi_{4.15}Fe_{0.85}$. In that Phase, the malfunction of the cold side alloy prevented the achievement of the design refrigeration capacity and cooling temperature.

In Phase III, a new batch of the cold side alloy, $MmNi_{4.15}Fe_{0.85}$, was loaded into the heat exchanger/containment vessel. Test results in this Phase showed that the actual hydride utilization factor for the warm side alloy, $LaNi_5$, is 76.4% and for the cold side alloy, $MmNi_{4.15}Fe_{0.85}$, the factor is 63.7 percent (Table 8).

The warm side alloy, $LaNi_5$, is still the original batch; this alloy functioned as expected and there was no need to replace it. The improvement of 76.4% over the 72% previously reported factor for the $LaNi_5$ can be attributed to a small percentage of continued hydride activation over time.

The cold side alloy, $MmNi_{4.15}Fe_{0.85}$, while still below the estimate, showed a major improvement from 19% to 63.7%. This is a direct result of utilizing a new batch of this hydride in the heat exchanger vessel. It is difficult to

Table 8

Hydride Utilization Factors

Hydride Alloy	Assumed Factor	Previously Reported Factor (Ref. 5)	Actual Factor
$LaNi_5$	75%	72%	76.4%
$MmNi_{4.15}Fe_{0.85}$	75%	19%	63.7%

assess, however, the reason why the cold side alloy does not become more active than 63.7%. This may be the maximum to expect from the alloy or it could mean that, although utmost care was taken, contamination occurred at some point in the loading procedure. Nevertheless, testing continued and capacity and COP calculations were adjusted to reflect the actual hydride utilization factors.

4.3 SENSIBLE HEAT

The overall goal of the hydride heat exchanger design study is to increase the heat transfer between the hydride powder and the heat transfer fluid. With an increase in heat transfer, the cycle time is minimized. This in turn reduces the amount of hydride material necessary to produce useful output. High heat transfer can be accomplished with massive large surface area heat exchangers, but the hydride heat exchangers were tested in a heat pump mode and this is a cyclical device. There exist in cyclical devices parasitic thermal losses caused by the alternating heating and cooling of the heat exchanger and containment structure. These are referred to as sensible heat losses and they must be minimized or a valuable percentage of time and energy during each cycle will be used to overcome these losses.

The sensible heat losses that can be calculated include the losses to all the components that come in direct contact with the hydride powder. Referring to Figure 22, these components include the finned copper tubing, the aft plate and the insulation surface contacting the hydride. Also included in the calculation estimate of sensible heat is the copper U-tubes and the hydride powder. Although each heat exchanger vessel is identical, they contain different amounts of powder which results in a different estimate of sensible heat per vessel. The estimates were 1.63 Btu°F for the WSV and 1.81 Btu/°F for the CSV.

The finned copper tube heat exchanger was optimized for minimal sensible heat loss with maximum heat transfer in Phase I of this project. The remainder of the containment structure was not optimized for minimal sensible heat due to time and funding constraints. Therefore, the actual sensible heat losses are much greater than estimated. These losses are to the insulation vessels,

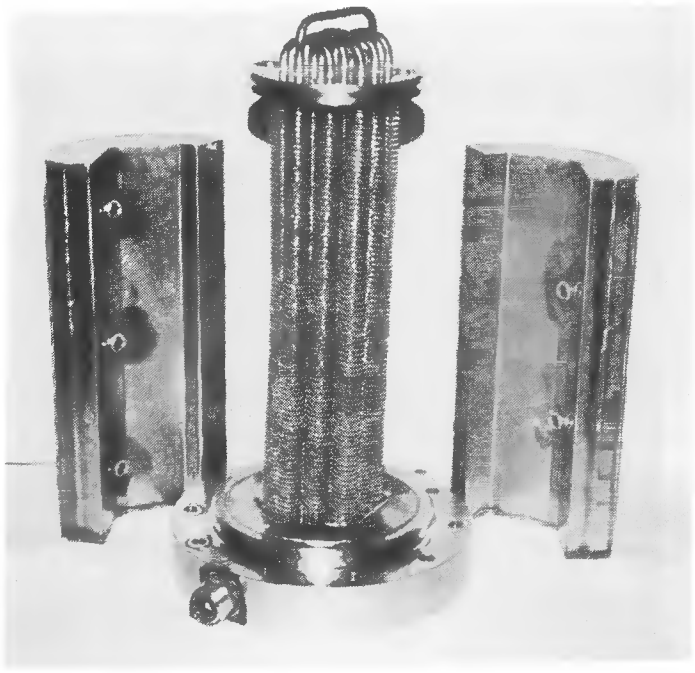

Figure 22. Hydride Heat Exchanger Device

flange heads and pressure vessel bodies. The experimental testing showed that with reference to the estimated sensible heat the actual sensible heat loss (Table 9) is 45% greater for the WSV and 64% higher for the CSV. These losses directly effect the capacity and COP and, therefore, are critical to the overall evaluation of the hydride heat exchangers. It is important to note that if the entire design had been optimized for sensible heat losses rather than only the finned copper tube heat exchange device, then the actual sensible heat losses would be less and the actual performance would have been much greater. The fact that the remaining sensible heat losses, as shown in Table 9, are dissimilar for each vessel can be attributed to the effect of different hydride amounts.

4.4 THERMAL MASS RATIO

The thermal mass ratio is defined as the ratio of the sensible heat loss of the hydride powder to the sensible heat loss of the entire structure including the hydride. Since, as previously mentioned, the total sensible heat is actually greater than estimated, then the thermal mass ratio is also effected. The actual thermal mass ratios (TMR) are:

$$\text{Actual WSV TMR} = \frac{SH_{LaNi_5}}{\text{Total SH}} = \frac{0.89 \text{ Btu/°F}}{2.367 \text{ Btu/°F}} = 0.38$$

Table 9

Actual Sensible Heat Losses

	Warm Side Vessel	Cold Side Vessel
Total sensible heat, actual experimental results - Btu/°F	2.367	2.960
Sensible heat loss to components in contact with hydride powder (including hydride powder) - Btu/°F	1.63	1.81
Remaining sensible heat loss to insulation vessels, flange heads and pressure vessel bodies - BTU/°F	0.737	1.15

$$\text{Actual CSV TMR} = \frac{SH_{MmNi_{4.15}Fe_{0.85}}}{\text{Total SH}} = \frac{1.07 \text{ Btu/°F}}{2.96 \text{ Btu/°F}} = 0.36$$

These figures, which are less than the estimated values of 0.55 for the WSV and 0.59 for the CSV, are a direct result of the low total sensible heat estimate. If the sensible heat losses to the hydride containment structure had been controlled, the actual thermal mass ratios would have been higher.

4.5 CYCLE TIME, CAPACITY AND COP

The cycle time, refrigeration capacity and COP of the hydride heat exchange devices are all interconnected heat transfer properties. Each is very dependent upon the hydride utilization factors and sensible heat losses as was described in Sections 3.1.5 through 3.1.7. Tables 6 and 7 described the characteristics of each test. Table 10 summarizes these results and compares the actual data to the predicted performance. In addition, because of the critical dependence of sensible heat upon the performance outcome, a column was added to the table to show the percentage of the cycle time used to overcome the sensible heat losses before energy was even transferred to the hydride.

As can be seen from the table, the shorter the half-cycle time, the higher the time percentage to overcome the sensible heat. This is critical because it has a detrimental effect upon the output capacity and COP. This is

Table 10

Analysis of Test Results

Half-Cycle Time (Minutes)	Estimated Refrigeration Capacity (Btu/Min) (from Table 4, Col.C)	Actual Refrigeration Capacity (Btu/Min)	Estimated COP (from Sec. 3.5.2)	Actual COP	% of Cycle-Time Used to Overcome Sensible Heat
2	91	20	0.17	0.09	16
3	60	33	0.17	0.13	12
4	45	35	0.17	0.15	6
5	36	25	0.17	0.14	5
8	23	29	0.17	0.18	2

especially evident in the two minute half-cycle time regime. The actual refrigeration capacity is only 22% of the estimated capacity.

The capacity does improve in the four and five minute half-cycle time ranges because the time percentages to overcome the sensible heat are much less. In these two cases the actual capacity is 78% of the estimated for a four minute half-cycle and 69% for a five minute half cycle. The actual COP is very close to the estimate.

In the eight minute half-cycle time, the sensible heat loss does not have as significant an impact. Only 2% of the cycle time was used to overcome the sensible heat and the capacity and COP values actually exceed the estimates.

5

HYDRIDE HEAT TRANSFER CONCEPT COMPARISONS

In the design of the hydride heat exchanger, heat transfer between the hydride particles and the heat transfer fluid is considered to be the key technical study area. Testing of this project's design was accomplished in a metal hydride heat pump mode and the heat exchange device was designed with this testing technique in mind. A hydride heat pump is a cyclical device and the parasitic sensible heat losses due to heating and cooling reduce the net useful output energy. Therefore, the design of the heat exchange device must minimize the sensible heat losses. This is accomplished by minimizing the heat exchange structure mass as well as the mass of the surrounding containment structure.

In addition, due to the expense of the hydride alloys, it is also necessary to reduce the amount of hydride material needed to produce useful output. This is achieved by minimizing the cycle times which is accomplished by increasing the rate of heat transfer to and from the heat transfer media and the hydride particles. In summary, the project goal was the design of a heat exchange device that produced high heat transfer with a low thermal mass.

The device used to fulfill this project's development goal has been thoroughly described throughout this report as well as in References 4 and 5. This section is devoted to an evaluation of other hydride heat transfer concepts. This includes characterizations in terms of potential for heat transfer, ease of manufacturing, structural integrity, component replacement, hydride containment, allowance for hydride expansion and hydrogen flow path properties.

The method used to evaluate these hydride heat transfer concepts is qualitative not quantitative. Table 11 is a catalogue of many of the heat transfer ideas that have been gathered from literature. Each concept has been judged in each of the seven categories mentioned above by stating whether that design is at an advantage (A), disadvantage (D) or unknown vantage point (U) in that category.

The heat transfer potential of each design was evaluated based on a perception of extended surface heat transfer. Many of these ideas were studied in Phase I of this project and were compared and rejected based on the superior possibilities of the finned copper tube heat exchanger.

The ease with which each design could be produced and manufactured is also an important consideration. Tubular components are the most uncomplicated to create except when consideration is given to inclusion of the filter component in the design. This is added complexity and requires a lot of handwork. Compressed or sintered hydride matrices are also difficult designs to fabricate.

Table 11

Hydride Heat Transfer Concepts

HYDRIDE HEAT EXCHANGE CONCEPT	DESCRIPTION	CHARACTERISTICS (A = advantage, D = disadvantage, U = unknown)						
		Heat Transfer	Ease of Manufacturing	Structural Integrity	Component Replacement	Hydride Containment	Hydride Expansion	Hydrogen Flow Path
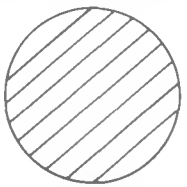	METALLIC TUBE CONTAINING HYDRIDE ALLOY WITH END FILTERS	D	A	D	A	A	D	D
	METALLIC TUBE CONTAINING HYDRIDE ALLOY AND A METALLIC FOAM WITH END FILTERS	A	D	A	A	A	A	D
	METALLIC TUBE CONTAINING HYDRIDE ALLOY AND A METALLIC FOAM WITH A LONGITUDINAL FLAT FILTER	A	D	A	A	U	A	A
	METALLIC TUBE CONTAINING HYDRIDE ALLEY AND A METALLIC FOAM WITH A CENTRAL CYLINDRICAL FILTER	A	D	U	A	A	A	U
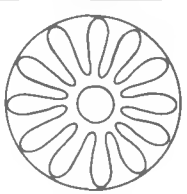	METALLIC TUBE WITH A CORRUGATED METALLIC FOIL FORMING INTERNAL FINS CONTAINING HYDRIDE ALLOY AND A CENTRAL CYLINDRICAL FILTER	A	D	D	A	A	A	U

Table 11 (Continued)

HYDRIDE HEAT EXCHANGE CONCEPT	DESCRIPTION	CHARACTERISTICS (A = advantage, D = disadvantage, U = unknown)						
		Heat Transfer	Ease of Manufacturing	Structural Integrity	Component Replacement	Hydride Containment	Hydride Expansion	Hydrogen Flow Path
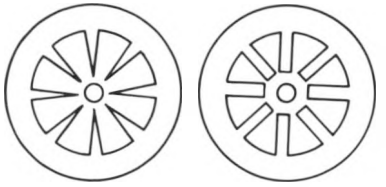	METALLIC TUBE WITH INTEGRAL INTERNAL FINS, CENTRAL CYLINDRICAL FILTER, CONTAINING HYDRIDE ALLOY	A	D	A	A	A	D	U
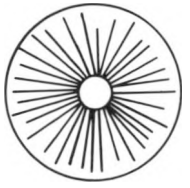	METALLIC TUBE WITH CENTRAL CYLINDRICAL FILTER AND A BOTTLE BRUSH TYPE DEVICE CONTAINING HYDRIDE ALLOY	A	D	A	A	A	A	U
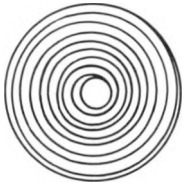	METALLIC TUBE WITH CENTRAL CYLINDRICAL FILTER AND SPIRAL WOUND METALLIC WIRE CLOTH CONTAINING HYDRIDE ALLOY	A	D	D	A	A	A	U
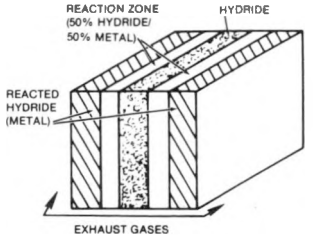	POROUS METALLIC-MATRIX HYDRIDE COMPOSITE (DESIGN IS BASED ON A COMPRESSED MIXTURE OF A HIGH THERMAL CONDUCTIVITY METAL AND A HYDRIDE ALLOY) — REF. 8	U	D	D	D	D	D	U

Table 11 (Continued)

HYDRIDE HEAT EXCHANGE CONCEPT	DESCRIPTION	CHARACTERISTICS (A = advantage, D = disadvantage, U = unknown)						
		Heat Transfer	Ease of Manufacturing	Structural Integrity	Component Replacement	Hydride Containment	Hydride Expansion	Hydrogen Flow Path
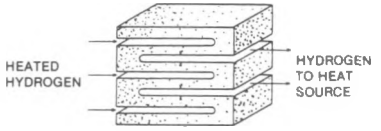	SINTERED HYDRIDE MATRIX (MIXTURE OF HYDRIDE ALLOY AND HIGH THERMAL CONDUCTIVITY METAL) — REF. 9	U	D	D	D	D	D	U
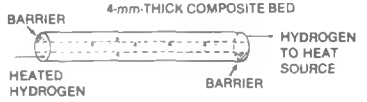	SAME AS ABOVE, EXCEPT IN A TUBULAR APPLICATION — REF. 9	U	D	D	A	D	D	U
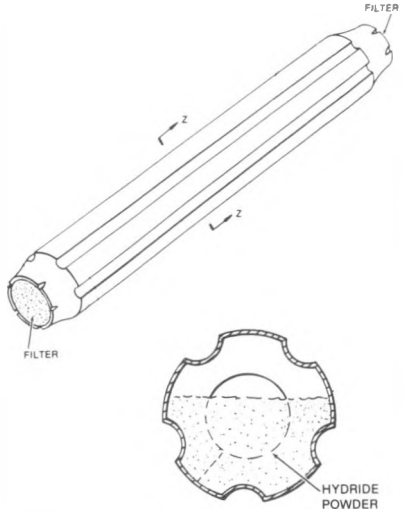	METALLIC FLUTED TUBE SECTION CONTAINING HYDRIDE POWDER WITH END FILTERS. REF. 10	D	D	A	A	A	D	D

Table 11 (Continued)

HYDRIDE HEAT EXCHANGE CONCEPT	DESCRIPTION	CHARACTERISTICS (A = advantage, D = disadvantage, U = unknown)						
		Heat Transfer	Ease of Manufacturing	Structural Integrity	Component Replacement	Hydride Containment	Hydride Expansion	Hydrogen Flow Path
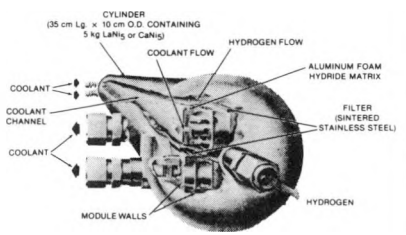	ADVANCED DESIGN ALUMINUM FOAM HEAT EXCHANGER REF. 7	A	D	U	D	A	A	A
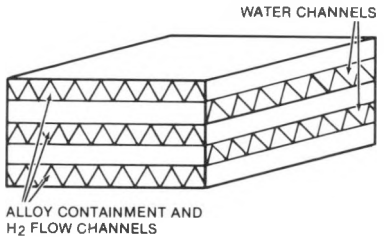	PLATE AND FIN HEAT EXCHANGER CONTAINING HYDRIDE ALLOY	A	D	D	D	A	A	D
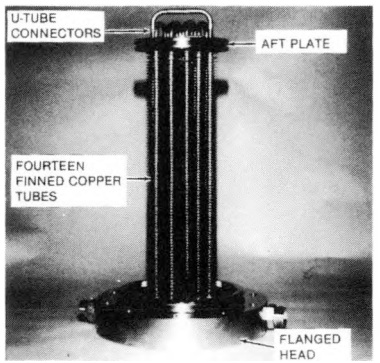	FINNED COPPER TUBE HEAT EXCHANGER (HYDRIDE STORED IN ANNULAR SPACING BETWEEN FINS)	A	A	A	A	A	A	A

Structural integrity refers to the ability of the design to withstand the cyclic effect of hydrogen absorption and desorption, i.e. the cycling between hydrogen evacuation and pressurization. Some of the internal heat exchange devices within the tubular component designs may distort or rupture with continuous cycling. In many of the designs, the orientation of the filter assembly could also be a source of limited lifetime by becoming clogged or crushed.

In a heat pump-type device, if all the hydride powder becomes contaminated or inoperable for some reason, the heat pump would fail. Therefore, the hydride is divided up into many different heat exchange/containment structures. In this way, if the hydride in one structure fails, the entire heat pump operation does not fail but can continue to operate at a reduced rate. Tubular components allow for easy component replacement, whereas a large single heat exchange component does not.

Containment of the hydride within the heat exchanger is a direct effect of the filter design. It is important that the hydride particles do not travel along with the hydrogen gas as the gas is cycled between alloys. Therefore, the designs were evaluated based on the inclusion of a filter in the design.

The process of hydrogen absorption and desorption causes the metal hydride crystal lattice to expand and contract leading to the comminution of the original hydride alloy particles. After many such cycles, the process of comminution produces a progressively greater proportion of fine particles. This also can create an internal pressure especially if void space is not allocated to accept the expanding particles. The heat transfer designs were evaluated based on the ability to adjust to this hydride expansion.

The path the hydrogen gas must follow between hydride vessels must be as short as possible and free of any potential gas flow restrictions. This allows the hydrogen to transfer between vessels as quickly as possible. The hydrogen flow path potential was also evaluated for each heat transfer design.

6

CONCLUSIONS AND RECOMMENDATIONS

Phase III of a three phase development project to design, fabricate and evaluate a heat/mass flow enhancement device for a metal hydride assembly has been completed. The device used to accomplish the goal of increased heat transfer with low thermal mass is a finned copper tube heat exchanger. In this Phase III effort, the hydride heat exchangers were tested in the heat pump test mode and evaluated for performance. In addition, other hydride heat transfer techniques were tabulated and reviewed.

The primary Phase III results are:

- Metal hydride heat transfer technology has been greatly advanced with the development of the novel heat exchanger design.

- Hydride alloys, as-received from vendors, can substantially vary from batch to batch in the chemical composition of the alloy. This is critical to the operation of the hydride heat exchangers in the heat pump test mode as any variation in the alloy constituency can effect performance.

- Replacement of the original batch of $MmNi_{4.15}Fe_{0.85}$ in the cold side vessel allowed for much improved heat pump operation in terms of capacity and COP.

- The actual hydride utilization factors were 76.4% for the warm side alloy, $LaNi_5$, and 63.7% for the $MmNi_{4.15}Fe_{0.85}$, the cold side alloy. The predicted value was 75% for both sides.

- The sensible heat losses were much greater than anticipated due to the unoptimized design of the insulation, the pressure vessel body and the flange head. (The project scope did not include optimization of these items.)

- Once actual sensible heat losses and hydride utilization factors were established, the method of predicting performance was accurate and reliable.

- All reporting requirements have been met.

- The program was completed within the original budget.

Based on these results and the experimental test data, the primary recommendation for this program is:

- In order to achieve optimum refrigeration capacity and COP when testing the hydride heat exchangers in the heat pump test mode, the sensible heat of the containment structure must also be minimized and optimized rather than just the finned copper tube heat exchange device.

REFERENCES

1. van Mal, H. H., Buschow, K. H. J. and Miedema, A. R., "Hydrogen Absorption in $LaNi_5$ and Related Compounds: Experimental Observations and Their Explanation", J. Less Common Metals , 35 (1974), pp. 65-76.

2. Sandrock, G. D., "Development of Low Cost Nickel-Rare Earth Hydrides for Hydrogen Storage", Proc. 2nd World Hydrogen Energy Conference, Zurich, Switzerland, Vol. 3 (1978).

3. Ozisik, M.N., Basic Heat Transfer, McGraw-Hill Book Company, 1977.

4. Argabright, T.A., "Metal Hydride/Chemical Heat Pump Development Program - Phase I Final Report", Solar Turbines Incorporated, under Contract No. 534098-S for Brookhaven National Laboratory, (1982).

5. Argabright, T. A., "Heat/Mass Flow Enhancement Design for a Metal Hydride Assembly - Phase II Final Report", Solar Turbines Incorporated, under Contract No. 534098-S for Brookhaven National Laboratory, (1983).

6. Huston, E. L. and Sandrock, G. D., "Engineering Properties of Metal Hydrides", J. Less Common Metals, 74 (1980), pp. 435-443.

7. Sheft, Irving, et. al., HYCSOS: A Chemical Heat Pump and Energy Conversion System Based on Metal Hydrides - 1979 Status Report, Argonne National Laboratory Report ANL 79-8, April 1979.

8. Moshe, Ron, "Metal Hydrides of Improved Heat Transfer Characteristics", Proceedings of the 11th Meeting of IECEC, 1979, p. 954 - 960.

9. Steyert, W. A., "New Heat Transfer Geometry for Hydride Heat Engines and Heat Pumps", Los Alamos Scientific Laboratory Paper No. LA-7822, (1978).

10. Turillon, Pierre P., U.S. Patent No. 4,135,621, Hydrogen Storage Module, January 23, 1979.

☆U.S. GOVERNMENT PRINTING OFFICE: 1985 515 034 10017